Immunity
Resource

Molecular Signature of CD8+ T Cell Exhaustion during Chronic Viral Infection

E. John Wherry,[1,3,*] Sang-Jun Ha,[1] Susan M. Kaech,[1,4] W. Nicholas Haining,[2] Surojit Sarkar,[1] Vandana Kalia,[1] Shruti Subramaniam,[1] Joseph N. Blattman,[1,5] Daniel L. Barber,[1,6] and Rafi Ahmed[1,*]
[1]Emory Vaccine Center and Department of Microbiology and Immunology, Emory University School of Medicine, 1510 Clifton Road Room G211, Atlanta, GA 30322, USA
[2]Departments of Pediatric Oncology and Medical Oncology, Dana-Farber Cancer Institute, Boston, MA 02115, USA
[3]Present address: Immunology Program, The Wistar Institute, 3601 Spruce Street Room 251, Philadelphia, PA 19104, USA.
[4]Present address: Section of Immunobiology, Yale University Medical School, New Haven, CT 06520, USA.
[5]Present address: Fred Hutchinson Cancer Research Center, Seattle, WA 98109, USA.
[6]Present address: Laboratory of Parasitic Diseases, NIH, Building 50, Room 6140, MSC 8003, Bethesda, MD 20892, USA.
*Correspondence: jwherry@wistar.org (E.J.W.), ra@microbio.emory.edu (R.A.)
DOI 10.1016/j.immuni.2007.09.006

SUMMARY

Chronic viral infections often result in T cell exhaustion. To determine the molecular signature of exhaustion, we compared the gene-expression profiles of dysfunctional lymphocytic choriomeningitis virus (LCMV)-specific CD8+ T cells from chronic infection to functional LCMV-specific effector and memory CD8+ T cells generated after acute infection. These data showed that exhausted CD8+ T cells: (1) overexpressed several inhibitory receptors, including PD-1, (2) had major changes in T cell receptor and cytokine signaling pathways, (3) displayed altered expression of genes involved in chemotaxis, adhesion, and migration, (4) expressed a distinct set of transcription factors, and (5) had profound metabolic and bioenergetic deficiencies. T cell exhaustion was progressive, and gene-expression profiling indicated that T cell exhaustion and anergy were distinct processes. Thus, functional exhaustion is probably due to both active suppression and passive defects in signaling and metabolism. These results provide a framework for designing rational immunotherapies during chronic infections.

INTRODUCTION

After acute infection, naive antigen-specific CD8+ T cells become activated, proliferate, acquire effector functions, and differentiate into effector CD8+ T cells. Most effector CD8+ T cells die by apoptosis, but ~5%–10% survive and differentiate into memory CD8+ T cells. These memory CD8+ T cells downregulate some properties of effector CD8+ T cells but retain the capacity to rapidly reactivate effector functions upon antigen encounter (Wherry and Ahmed, 2004). Memory T cells also undergo rapid proliferation upon re-exposure to antigen. In addition, memory T cells can survive and persist long term in the absence of antigen and acquire the ability of "self-renewal" by undergoing homeostatic proliferation in response to IL-7 and IL-15 (Surh et al., 2006; Wherry and Ahmed, 2004). This combination of antigen-independent persistence and the ability to rapidly reactivate effector functions allows memory CD8+ T cells to confer robust long-term protective immunity.

During many chronic infections, in contrast, severe defects in CD8+ T cell responses develop, and virus-specific CD8+ T cells often fail to differentiate into memory CD8+ T cells (Shin and Wherry, 2007). CD8+ T cell exhaustion was first described with chronic LCMV infection of mice during which virus-specific CD8+ T cells persist but lack effector function (Zajac et al., 1998). During chronic LCMV infection, virus-specific CD8+ T cells initially develop the ability to perform effector functions. These functions are lost, however, in a hierarchical manner during chronic infection with some functions that are exhausted early (e.g., IL-2, cytotoxicity, and proliferation), whereas others (e.g., IFN-γ) persist longer (Wherry et al., 2003). Eventually, especially if viral load is high and CD4+ help is lacking, virus-specific CD8+ T cells fully lacking effector functions are found (Fuller and Zajac, 2003; Ou et al., 2001; Wherry et al., 2003). Similar types of dysfunction have also been described in other experimental models of viral infection, during human chronic infections and during cancer (Shin and Wherry, 2007).

CD8+ T cell exhaustion during persisting infection is likely to have an important impact on viral control, and some of the underlying mechanisms for this dysfunction are beginning to be elucidated. Recently, we have found that the inhibitory receptor PD-1 is an important pathway regulating CD8+ T cell exhaustion during chronic LCMV infection in mice (Barber et al., 2006). Blockade of the PD-1:PD-L pathway during chronic LCMV infection leads to recovery of T cell function and reduced viral load (Barber et al., 2006). These results have been extended to primates and humans in which the PD-I:PD-L1 pathway also regulates function of SIV-, HIV-, and HCV-specific T

cells in vitro (Day et al., 2006; Petrovas et al., 2006; Petrovas et al., 2007; Radziewicz et al., 2006; Trautmann et al., 2006; Urbani et al., 2006; Velu et al., 2007; Zhang et al., 2007). Our previous studies identified the importance of the PD-1:PD-L pathway during chronic infection by using a gene-expression profiling approach (Barber et al., 2006). IL-10 has also been recently implicated in $CD8^+$ T cell dysfunction during chronic viral infection (Brooks et al., 2006; Ejrnaes et al., 2006). It is likely, however, that pathways in addition to PD-1 and IL-10 influence $CD8^+$ T cell function and differentiation during persisting infections. In this study, we report the analysis of global gene-expression profiles for virus-specific exhausted $CD8^+$ T cells.

We have examined the molecular signature of $CD8^+$ T cell exhaustion by using the well-characterized model of chronic LCMV infection. We have compared the gene-expression profiles of exhausted LCMV-specific $CD8^+$ T cells to those of functional LCMV-specific effector and memory $CD8^+$ T cells generated after acute infection. This approach revealed key insights into the biology of $CD8^+$ T cell dysfunction during chronic infection. First, exhausted $CD8^+$ T cells overexpressed multiple cell-surface inhibitory receptors, in addition to PD-1. Second, the fact that transcription of genes encoding molecules involved in signaling from TCR and cytokine receptors was downregulated probably compromised the efficiency of these pathways. Third, many genes for chemotaxis, migration, and adhesion were changed in exhausted $CD8^+$ T cells. Fourth, exhausted $CD8^+$ T cells displayed a dramatically altered pattern of differentiation compared to effector and memory $CD8^+$ T cells including a distinct expression pattern of transcription factors. Fifth, $CD8^+$ T cell exhaustion was associated with profound translational, metabolic, and bioenergetic deficiencies. Finally, exhausted $CD8^+$ T cells possessed a gene-expression profile distinct from that reported for anergic T cells. It is likely that the defects in effector functions in exhausted $CD8^+$ T cells are due to both active suppression, for example by inhibitory receptors, and passive defects in signaling and metabolism. The defects and altered pathways identified in exhausted $CD8^+$ T cells provide an important framework from which to begin dissecting the control of $CD8^+$ T cell differentiation when pathogens persist and suggest novel potential targets of therapeutic intervention during chronic infections.

RESULTS

Function and Phenotype of Exhausted $CD8^+$ T Cells

To address the molecular mechanisms of $CD8^+$ T cell exhaustion, we compared the gene-expression profiles of exhausted LCMV-specific $CD8^+$ T cells from chronic infection to fully functional LCMV-specific effector and memory $CD8^+$ T cells generated after acute LCMV infection. Infection with the Armstrong strain (Arm) of LCMV causes an acute infection that is cleared by day 8–10 p.i., resulting in the generation of functional effector and memory $CD8^+$ T cells (Ahmed et al., 1984). In contrast, the clone 13 strain of LCMV causes a chronic infection with loss of effector functions (exhaustion) and ineffective viral control (Ahmed et al., 1984; Wherry et al., 2003; Zajac et al., 1998). In the present study, we have used chronic LCMV infection of $CD4^+$ T cell-depleted mice because these conditions result in the most profound $CD8^+$ T cell exhaustion and we wanted to gain an understanding of the molecular pathways involved in highly dysfunctional virus-specific $CD8^+$ T cells. The main features of exhaustion, however, are preserved in $CD4^+$ T cell-sufficient mice (Wherry et al., 2003; Zajac et al., 1998). LCMV Arm infection or clone 13 infection resulted in similar viral replication in the spleen 3 days p.i. (Figure 1). LCMV Arm is completely cleared by day 8–10 p.i., whereas replication of clone 13 continues at a high level for life in $CD4^+$ T cell-deficient mice ([Figure 1] and Zajac et al. [1998]). In contrast to functional effector and memory $CD8^+$ T cells generated after Arm infection, exhausted $CD8^+$ T cells during clone 13 infection were nonfunctional and unable to produce substantial levels of IFN-γ and TNF-α upon peptide stimulation (Figures 1B–1D). It is important to point out that the studies of gene-expression profiling described below were performed on antigen-specific effector, memory, and exhausted $CD8^+$ T cells of the same antigen specificity (e.g., the DbGP33 LCMV epitope).

Patterns of Gene Expression

To define the molecular signature of $CD8^+$ T cell dysfunction during chronic viral infection, we profiled the gene-expression patterns of effector, memory, and exhausted $CD8^+$ T cells by using Affymetrix U74A microarrays containing ~12,500 mouse genes. The gene-expression profiles of sorted effector, memory, and exhausted $CD8^+$ T cells were each compared to naive $CD8^+$ T cells so that direct comparisons between all three groups could be facilitated. An example of presort and postsort analysis of exhausted $CD8^+$ T cells is shown in Figure 2A. A total of 490 genes was upregulated or downregulated by at least 2-fold in the exhausted $CD8^+$ T cells (Figure 2B). The vast majority of genes (338) were differentially expressed only in the exhausted $CD8^+$ T cells.

There was more similarity in gene expression between exhausted and effector $CD8^+$ T cells compared to exhausted and memory $CD8^+$ T cells as revealed by both numerical representation of genes differentially expressed (Figure 2B) and gene clustering analyses (Figures 2C and 2D and Figure S1 in the Supplemental Data available online). This clustering analysis, however, also reveals a number of genes uniquely upregulated (n = 123) or downregulated (n = 135) in exhausted $CD8^+$ T cells, indicating that $CD8^+$ T cell exhaustion reflects a unique state of gene expression compared to that of naive, effector, and memory $CD8^+$ T cells.

A gene-expression signature could also be identified that uniquely defined naive, effector, memory, and exhausted $CD8^+$ T cells (Figure 2E). Some expression of the genes found in the effector signature was noted in the exhausted $CD8^+$ T cells. The panel of genes that identified exhausted $CD8^+$ T cells, however, was not present in

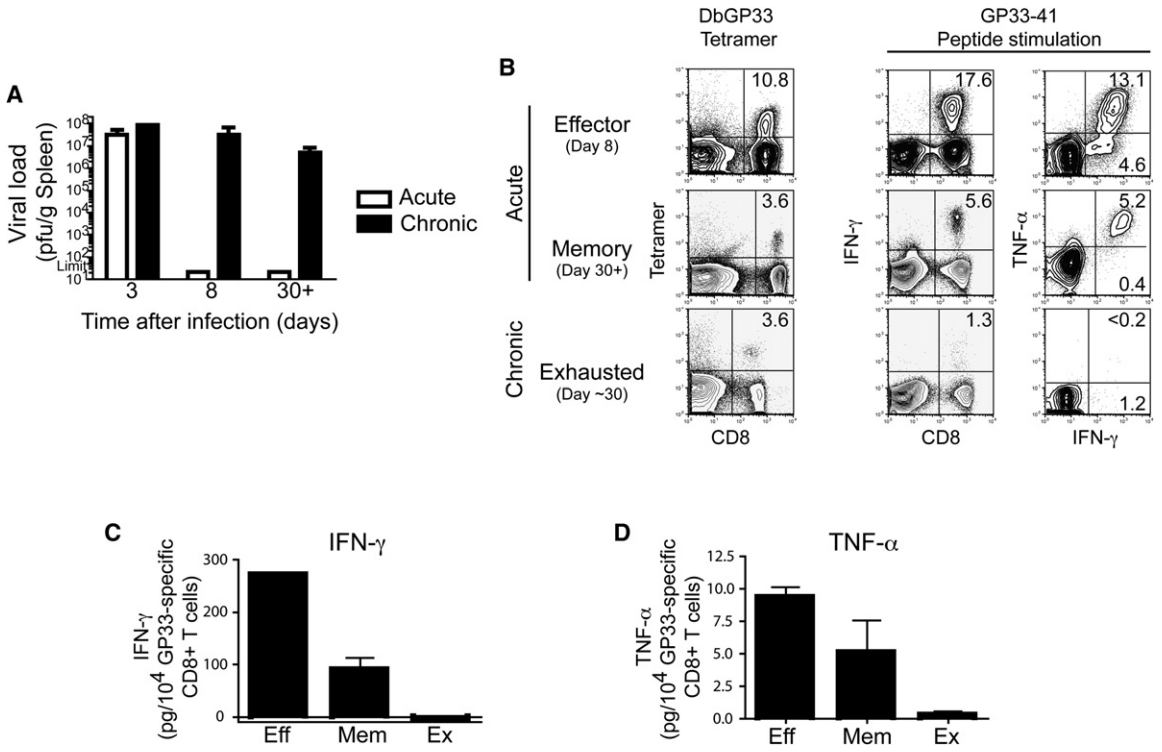

Figure 1. Characterization of Effector, Memory, and Exhausted LCMV-Specific CD8$^+$ T Cells

(A) LCMV in the spleen was quantified by plaque assay at the indicated time points after LCMV Arm and clone 13 infections. A similar pattern of viral load was also seen in other tissues (data not shown and Wherry et al. [2003]).

(B) DbGP33 tetramer staining was performed at effector and memory time points after Arm infection or clone 13 infection. ICS was performed for IFN-γ and TNF-α production. (Note that the higher frequency of cytokine producing effector and memory CD8$^+$ T cells is accounted for by the KbGP34 response that is deleted during chronic LCMV infection [Wherry et al., 2003].)

(C and D) Effector, memory, and exhausted CD8$^+$ T cells were stimulated for 5 hr, supernatants were collected, and IFN-γ (C) or TNF-α (D) concentrations were determined by ELISA. The amount of cytokine produced per 10^4 GP33-specific (both DbGP33 and KbGP34) CD8$^+$ T cells was calculated. Data are representative of five or more (A and B) experiments or two (C and D) independent experiments. Error bars represent SD.

any of the other three cell types, supporting the notion that exhaustion is a unique state of CD8$^+$ T cell differentiation. An advantage of the approach used in Figure 2E is that we isolated LCMV-specific CD8$^+$ T cells at multiple time points after acute infection to gain a kinetic portrait of gene expression during memory CD8$^+$ T cell differentiation similar to previous studies (Kaech et al., 2002). With this analysis, it is clear that the similarities between exhausted and effector CD8$^+$ T cells do not persist after day 8 of acute infection, suggesting that the patterns of memory T cell differentiation and exhaustion diverge or differ substantially as functional CD8$^+$ T cells differentiate into memory CD8$^+$ T cells.

Gene-Expression Signatures of CD8$^+$ T Cell Exhaustion

To begin to identify the molecular pathways associated with CD8$^+$ T cell exhaustion, we identified genes that differed in expression by more than 2-fold by microarray analysis. (Table 1 and Tables S2–S5). The gene-expression profiles of exhausted CD8$^+$ T cells were also compared directly to that of effector (Table S2) and memory (Table S3) CD8$^+$ T cells. A subset of samples was also hybridized to the U74Bv2 and U74Cv2 Affymetrix microarrays containing an additional ~25,000 mouse genes and ESTs (Table S4). The major findings from the data shown in Table 1 and Tables S2–S5 are outlined below.

Overexpression of Inhibitory Receptor Genes during Exhaustion

One of the more striking results from the gene-expression profiles was the overexpression of mRNA for cell-surface molecules known or suspected to have inhibitory activity. We have recently identified PD-1 as a major cell-surface inhibitory receptor capable of regulating CD8$^+$ T cell exhaustion (Barber et al., 2006). In the current analysis, in addition to PD-1, 13 other potentially inhibitory cell-surface pathways were identified, and most of these molecules were specifically overexpressed in exhausted CD8$^+$ T cells (Table 1 and Tables S2, S3, and S5). These inhibitory receptors included those with well-described inhibitory function such as 2B4 (Assarsson et al., 2005), Ly49 family members (Klra7 also known as Ly49D-GE, Klra3 also known as Ly49c) (Lanier, 1998), and GP49B (Katz et al., 1996; Rojo et al., 1997). Molecules with less well-characterized but potential inhibitory capacity were

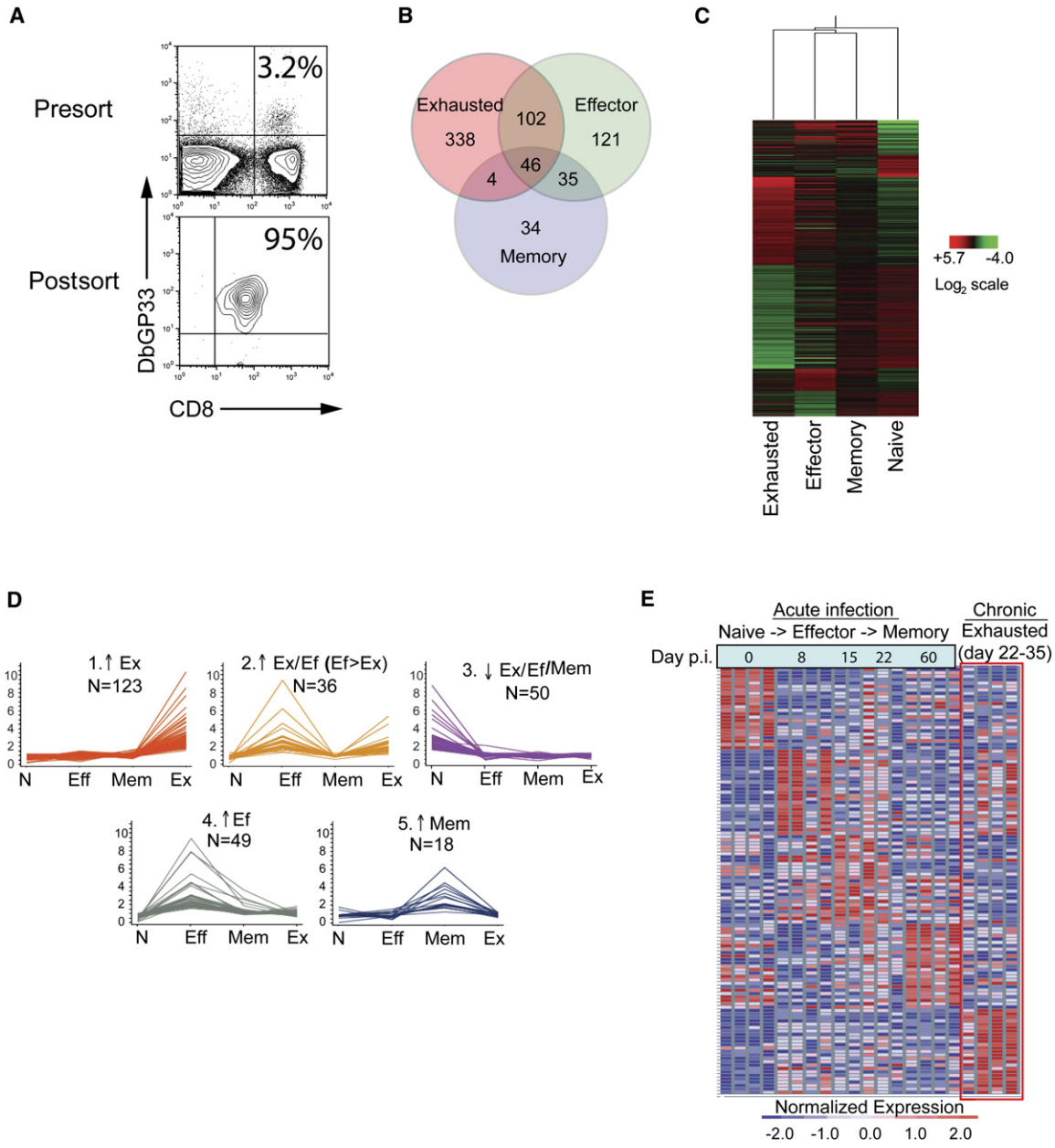

Figure 2. Gene-Expression Profiles of Effector, Memory, and Exhausted CD8$^+$ T Cells Compared to Naive CD8$^+$ T Cells

(A) Presort and postsort analysis of exhausted LCMV-specific CD8$^+$ T cells. The upper panel indicates the percentage of CD8$^+$ T cells presort.

(B) The number of genes differentially expressed by the different LCMV-specific CD8$^+$ T cell populations on the basis of Affymetrix U74A microarrays is shown.

(C) K means-cluster analysis of the gene-expression profiles of naive, effector, memory, and exhausted CD8$^+$ T cells indicating the relatedness of the populations.

(D) K means-clustering identifying individual clusters of gene expression for the exhausted, effector, memory gene-expression profiles. Examples of five such clusters out of 15 are shown. Additional clustering data is provided in Figure S1 and a full list of genes in each cluster is given in Table S1.

(E) Clustering analysis for a panel of genes that identifies each CD8$^+$ T cell population. Naive (acute infection day 0; n = 4), effector (acute infection day 8; n = 4), and memory (acute infection day 60, n = 4) are indicated. In addition, day 15 (n = 2) and day 22 (n = 3) time points from acute infection are also included. The cluster of genes from exhausted CD8$^+$ T cells (n = 4 samples) is also shown.

also overexpressed by exhausted CD8$^+$ T cells including CD160 (Maeda et al., 2005), Ptger4 (Kabashima et al., 2002), and LAG-3 (Workman et al., 2002).

The CD28:CTLA-4 family contains three related inhibitory receptors that can be expressed by T cells: CTLA-4, PD-1 and BTLA (Greenwald et al., 2005). PD-1 was

Table 1. Gene-Expression Profiles of Exhausted, Effector, and Memory T Cells compared to Naive CD8 T Cells

Gene	Ex N	Eff N	Mem N	Acc. #	Other Names
I. Inhibitory receptors					
Gp49b	12.24	4.29	4.48	M65027	
Cd244	11.02			L19057	2B4
Ctla4	6.93	2.30	2.33	X05719	
Pdcd1	6.55			X67914	PD-1
Cd160	4.08			AF060982	
Klrc1		4.41	2.03	AF095447	NKG2A
Pigerr4	4.07			D13458	
Gp49b	4.04	2.56	2.49	U05265	
Lag3	3.25			X98113	
Klra9	2.88	2.04		U49866	Ly49D-GE
Klrg1	2.59	36.90	7.36	AF097357	
Klra3	2.20			U56404	Ly49c
Ptger2	2.08			AB007696	
II. Cell surface receptors and ligands					
Tnfsf6	16.29	6.12	5.61	U06948	FasL
Ctla2b	8.64	14.44	11.60	X15592	
Ctla2a	8.30	12.72	12.77	X15591	
Itgax		7.60	3.07	AI035495	CD11c
Nrp	5.65			D50086	neuropilin 4-1BB
Tnfrsf9	5.42			AA798611	
Pglyrp1	5.01			AV092014	
Tmem49	4.62	2.79		AW122274	
Il18r1		4.21	4.93	U43673	
Klrk1		4.05	3.86	AF030313	NKG2-D
Adam19	3.80	2.37		AA726223	
Itga4		3.75		X53176	CD49d
Klrk1		3.58	2.56	AF054819	NKG2-D
Ly6c		3.56	2.79	D86232	
Itgb1	3.52	3.94	3.61	X15202	CD29/VLA4
Tnfrsf1b	3.48			X87128	TNFr p75
Ly6a	3.24	4.06	4.07	X04653	
Alcam	2.92			L25274	CD166
Cd9	2.60			L08115	
Pglyrp1	2.50			AF076482	
Igsf10		2.48		AA536958	
Cd7	2.45			D31956	
Glycoprot	2.38			Z22552	
Itga4	2.35	4.35		AA189389	CD49d VLA1
Tnfrsf1a	2.31			AV252882	TNFr p55
Cd48		2.26		X53526	
Itgb2		2.26		M31039	CD18
Fcgr2b		2.23	2.45	M31312	
Ifitl1		2.19		D13695	
Itgav	2.18			AI843901	CD51
Itgb1	2.17			X15202	CD29
Gpr65	2.12			U39827	
Crtam			2.11	AF001104	
Mox2	2.03			AF029215	
Cd79b			-2.00	J03857	
Cd1d1	-2.02			M63697	
Itm2a		-2.06		L38971	
Sema4b		-2.07		AA266467	
Icam2	-2.09			X65493	
Itgae	-2.09	-2.08		AV268095	
Cd24a	-2.17		-2.46	M58661	
Sema4a	-2.26			X85991	
Il17r	-2.28			AI286698	
Cd6	-2.29			AJ006074	S1P4
Tm4sf13		-2.30		AI837621	
Itgae			-2.32	AV268095	
Lbr	-2.37			AW214587	
Ms4a1	-2.40	-2.42	-3.14	M62541	CD20
Cd72	-2.46	-3.70		J04170	
Klrd1	-2.49			AF030311	
Il17r	-2.56			U31993	
Tir6	-2.56	-3.25		AB020808	
Crlf3	-2.71			AF046060	
Ptprc	-2.74			M23158	
Il4ra	-2.82	-2.38		M27960	CD124
Ephb4	-3.13			U06834	
Sell	-3.14	-4.50		M36058	CD62L
Il7r	-3.52	-5.05		M29697	CD127
Itgb7	-3.70			M68903	
Il6ra	-4.15	-3.91	-2.58	X51975	
Vcam1		-4.20		M84487	
Itgae	-5.56	-5.56	-5.71	U12236	
III. Homing and migration					
Ccr5	42.08	32.63	21.29	AV370035	
Ccl5	23.45	30.80	22.87	AF065947	
Ccr2		16.65	5.77	U56819	
Ccl3	10.69			J04491	
Ccl4	4.01			X62502	
Ccr5	3.48	7.83	4.98	AF022990	
Cxcr3	3.05	4.52	5.82	AI045145	
Ccr5		2.62		X94151	
Ccl9		2.03		U49513	
Ccr2	2.35			AF030185	
Cxcl10	2.06			M33266	
Ccr7	-5.99	-8.26	-2.36	L31580	
Cxcr4		-2.22		Z80112	
IV. MHC					
H2-Q7		2.85		M27134	
H2-Q10		2.62	2.98	X16426	
H2-Q8		2.13		D90146	
Tap2	-2.65	-2.69		AF027865	
H2-Eb1			-2.06	X00958	
H2-Aa		-2.16	-3.92	X52643	
Ii			-3.06	X00496	
V. Glycosylation					
Lgals1		15.96	5.18	X15986	
Lgals3		5.30		X16834	galectin-3
Lgals1	5.22			X15986	
Lgals3	4.00			X16834	galectin-3
Siat10		2.79	3.58	AI153959	
St6gal1	-9.09	-10.27	-8.06	AI117157	
VI. TGFß pathway					
Tieg1	2.13			AF064088	
Smad7		-2.01		AF015260	
Smad1	-2.68	-5.29		U58992	
Smad1	-2.96	-6.21		U58992	
VII. Effector functions					
Gzmb	15.09	27.75	5.13	M12302	
Gzma	11.18	19.50		M13226	
Gzmk	10.55	3.00	2.94	AF011446	
Ifng	9.13	6.35	17.20	K00083	
Gzmm			2.66	AB015728	
Prf1		2.62	2.24	X12760	
Ltb	-2.31			U16985	
VIII. Signaling					
S100a6	17.03	40.33	20.29	X66449	
Il18rap		6.37	3.09	AF077347	
Rgs16	5.75			AW349152	
S100a4	4.83	12.93	2.54	M36579	
Ptpn13	4.75			D83966	
Gpr56	3.85			AI841654	
S100a10			3.80	M16465	
Sh2d2a	3.64			AI646422	
Fyn	3.11	2.11		M27266	
S100a11	2.87	3.84		U41341	
S100a13	2.65	3.49		AV007820	
Rcn	2.55			D13003	
Rhoq	2.46	2.36		AW060401	
Plk4	2.43			L29480	
Prkwnk1	2.40			AV319920	
S100a13	2.31			AV067606	
Sh2d1a			2.31	AF097632	SAP
Tank	2.25			U59864	
S100a13	2.18	4.15		X99921	
Sh3bgrl	2.14	2.39		AI848671	
Racgap1		2.05		AW122347	
Gtpbp1	-2.00			U87965	
Lck	-2.01			M12056	
Peli1	-2.03	-2.34		AW124934	
Fkbp4	-2.09			X17069	
Gnb2-rs1	-2.17			D29802	
Itpr5		-2.21		AF031127	
Map4k4	-2.22			U88984	
Arhgap1	-2.22			AI846773	
Rgs10		-2.33		AV335997	
Arhgef1	-2.33			U58203	
Blk			-2.40	AA204265	
Ikbke	-2.44			AB016589	
Dtx1	-2.50	-2.03		U38252	
Tgtp	-2.51	-3.36		L38444	
Tec	-2.64	-2.71	-2.91	X55663	
Mapk8	-2.66			AW122136	
Pik3cd	-2.77			AW124359	
Rgs10	-2.81	-4.2		AI847399	
Gadd45a	-2.85			U00937	
Hcph	-2.92			M68902	Shp1
Pik3il	-3.18			Y17808	
Stk38	-3.25			AA691445	
Ramp1	-3.30	-3.76		AJ250489	
Il6st	-3.36			AI843709	
Socs3		-3.36		AV374868	
Dusp1		-3.47	2.60	X61940	
Dgka	-7.46	-2.36		AF085219	
Il6st		-7.94	-3.95	AI843709	
IX. Cytoskeleton					
Myo1f		2.91	2.39	X97650	
Kif11		2.19		AJ223293	
Tubb5	-2.07			X04663	
Tubb5	-2.21			X04663	
Actn1	-2.26	-5.18		AI195392	
Actn1	-2.43	-2.71	-2.64	AI195392	
Macf1	-2.44			AI843799	
Actb	-3.40	2.09		J04181	
Kif23			-2.22	AI591702	
X. IFN response					
Isg20	3.49			AW122677	
Mx1	2.86			M21038	
Irf4	2.32			U20949	
G1p2	2.28			AV152244	
Icsbp1	2.20			M32489	
Ifnar1		-2.04		M89641	
XI. Proteases					
Serpinb9		4.59		U96700	
Serpina3g	3.48			M64085	
Rnf11	2.70			AB024427	
Capn2		2.51		D38117	
Ctsd		2.39		X68378	catheo. D
Serpinb6a	2.35			U25844	
Serpinb9	2.32			U96700	
Mcpt5		2.13		M68898	
Serpina3g			2.13	M64085	
Ctsl	-2.02	-2.16		X06086	
Nedd4l		-2.12		AI840868	
Ctss		-2.14		AJ223208	catheo. S
Lyzs	-2.38		-2.22	M21050	
Prss19	-2.65			D30785	
XII. Antigen receptors					
Tcrg-V4	4.32			X00697	
Tcrg-V4	2.58			M18858	
Tcrb-V13	2.11			AF093870	
Igk-V28	-2.08			M18237	
Igk-V21	-2.31			M80423	
Igk-V28			-2.43	M18237	
Igk-V21			-2.55	M80423	
Iga	-3.08			J00475	
Iga		-3.13	-3.77	J00475	
Igh-6	-4.72	-3.29	-3.80	V00817	
Igh-6	-6.02	-5.13	-8.33	V00821	
Tcrd-D2J1	-11.67			L36135	
Igm-hc6			-2.58	AI183084	
XIII. DNA repair					
Top2a		4.11		U01915	
Rpa2	3.10			D00812	
Top2a	2.87			U01915	
Rpa2		2.28		D00812	
Dntt		-2.12	-2.33	AV312871	
Ddit4			-2.19	AI849939	
Dntt		-2.22	-2.38	X68670	
Ssbp2	-2.51	-3.86		AI837107	
XIV. Transcription					
Pbx3	13.97	2.03		AF020200	
Bhlhb2		12.44	7.55	Y07836	
Eomes	10.59	2.48	4.34	AW120579	
Hist1h2ac	7.84	3.91		M33988	
Bhlhb2	6.72			Y07836	
Foxb			6.60	X14897	
Ier5	5.85			AF079528	
Eomes	4.98		2.33	AB031037	
Hod		4.82	4.75	AW123564	
Nr4a2	4.29			U86783	Nurr1
Idb2	3.92	5.29	4.35	AF077861	
Prdm1	3.56	4.06		U08185	Blimp-1
Litaf	3.54			AI852632	
Klf4			3.49	U20344	
Nfatc1	3.14			AF087434	
Hmgb2	2.95	3.47		X67668	
Runx2	2.94	3.45	3.58	D14636	
Jak3	2.63			AV266650	
Tbx21		2.61		U53228	
Rora			2.61	U20735	
Junb			2.61	M63725	
Atf1	2.40			X99921	
Tfdp1	2.28			X72310	
H2afz		2.27		U70494	
Cebpb			2.22	M61007	
Nfil3	2.10			U83148	
Ndfip1	2.08			AI835257	
Zfp91	2.08			U05343	
Ezh2		2.02		U52951	
Zfp288		-2.00		AI987985	
Ets2	-2.00			J04103	
Nedd4l	-2.02			AI840868	
Bzw1	-2.03			AI852534	
Ets2		-2.04		J04103	
Gtf2i	-2.05			AF017085	
Hmgn1	-2.08	-2.84		X53476	
Fos	-2.11	-3.86	2.51	V00727	
Tcf12		-2.15		X64840	
Klf3	-2.18			U36340	
Tcf7	-2.24	-2.20		X61385	
Spred2		-2.29		AI851250	
Klf13	-2.34			AW125783	
Smc4l1		-2.35		AA032310	
Bzw2	-2.43			AW060951	Shp1
Myb		-2.44	-6.80	M12848	
Klf2	-2.50			U25096	
Smarca2	-2.51	-3.14		AI842968	
Myc		-2.86		L00039	
Klf3	-3.68			AI851658	
Nfe2l2	-3.79			U70475	
Tcf7	-3.86	-5.05		AI019193	
Lef1	-5.41			D16503	
Satb1	-5.85	-2.05		U05252	
XV. Apoptosis, cell death, caspases, and annexins					
Anxa1		13.17		M69260	
Casp3	8.77			U54803	
Anxa1		8.19		AV003419	
Anxa1			4.83	AV003419	
Bag3			3.55	AV373612	
Bcl2a1c	3.56	2.56		U23778	
Casp4	3.43			Y13089	
Bag3	3.41	2.77		AV373612	
Casp1	3.37	2.22	2.38	L28095	
Anxa1		3.25	6.13	M69260	
Anxa2	3.05	8.09	2.89	M14044	
Perp		2.85		AI854029	
Bcl2a1a	2.46	2.72		U23781	
Tnfaip3			2.25	U19463	A20
Casp3		2.08		U54803	
Pawr	2.02			AA260005	
Tnfaip8		-2.04		AI839109	
Bnip3l	-2.76			AF067395	
Bcl2		-4.63		L31532	
XVI. Membrane biology and vesicle transport					
Rasrl	8.63	2.49		D78354	
Rabgip1		2.21		AJ245569	
Vamp8	2.13			AF053724	
Snx10	2.02	4.94		AI746846	
Lamp1	-2.00			M32015	
Atp6v0a2	-2.05			AW049274	
Snx4	-2.08			AI838691	
Piga			-2.17	AV308550	
Pld3	-2.19			AF026124	
Elovl5	-2.62	-2.25		AI852098	
Rabac1	-2.87			L40934	
Piga	-3.46	-2.26	-2.35	D31863	
XVII. Cell Cycle					
Cks2	7.33			AA681998	
Mki67	5.51	7.61		X82786	Ki67
Cks2		3.43		AA681998	
Gas2	3.04			M21828	
Nusap1	2.73	2.16		AA275196	
Madl2l1	2.72	2.90		U83902	
Cdc6		2.69		AJ223087	
Chek1	2.49			AF016583	
Ccnb1	2.42	2.23		X64713	cyclin B1
Cdc2a	2.35	2.22		M38724	
Cks1		2.34		AB025409	
Prc1	2.30	2.99		AA856349	
Smc2l1	2.21			U42385	
Ccnb2	2.19	2.77		X66032	cyclin B2
Mki67	2.11			AV309347	
Clk		-2.03		M38381	
Skp1a	-2.04			Z47088	
Clk4	-2.05	-2.04		AF033566	
Clk2	-2.14			AF033564	
Gas5		-2.21		AI849615	
Ccnd2		-2.32		M83749	cyclin D2
Ccnd2	-2.36	-2.32		M83749	cyclin D2
Pak2	-2.38			AW122689	
Anapc5	-2.56			AI847314	
Gadd45a		-2.67		U00937	
XVIII. Metabolism					
Kcnj8			4.58	D88159	
Hba-a1		3.76		V00714	
Entpd1	3.72			AF037366	CD39
Aqp9			3.55	AA967194	
Apobec2		3.40		AW124988	
Car2	3.13			M25944	
Atp5l		2.93		Y17223	
Pfkp		2.83		AI853802	
Gpd2	2.77			D50430	
Clic4	2.60			AI845237	
Slc4a7	2.52	2.09		AI594427	
Art3	2.43			Y08027	
Odc			2.43	M12330	
Txndc5		2.37	2.01	AI841920	
Txn1	2.35	2.36		X77585	
Sec61g	2.33	3.01		U11027	
Ltb4dh		2.33		AA596710	
Rrm2	2.27			M14223	
Csda		2.27		D14485	
LOC14433	2.17	2.34		M32599	
Cpsf2	2.16			AW047563	
Glrx1	2.11	2.27		AB013137	
Ech1		2.26		AF030343	
Ndufa6		2.08		AW047339	
Ndufa5	2.00			AA823381	
Cmah	-2.00			D21826	
Prps1	-2.04			AB025048	
Gart		-2.04		U20892	
Ppic		-2.11	-3.04	M74227	
Apex1		-2.11		D90374	
Tmc6	-2.14			AI874754	
Hbb-b1	-2.23			V00722	
Hexa	-2.16			U05837	
Amd1		-2.24		D12780	
Hmgcs1	-2.28			AW124932	
Sfrs7		-2.28		AA711516	
Dntt	-2.30			X68670	
Acadm	-2.32			U07159	
Abce1	-2.33			U90446	
Hba-a1	-2.43			V00714	
Kcnn4	-2.43			AF042487	
Kctd10	-2.46			AI852623	
Dntt	-2.53			AV312871	
Mat2a	-2.53			AW124835	
Kctd12		-2.53		AI842065	
Pdha1	-2.56			M76727	
P2rx4		-2.64		AF089751	
Adcy7	-2.74			U12919	
Idh2	-2.76		-2.03	U51167	
Atp6v0b	-2.82			AI842889	
Sdha	-2.96			AI835718	
Hspa9a		-2.98		D17666	
Hbb-b1	-3.01	2.66		J00413	
Adh5	-3.02			M84147	
Scd1	-3.03	-2.82	-4.31	M21285	
Impdh2	-3.07			M33934	
Acaa2f	-3.58			AW125884	
Slc12a7	-3.80	-3.92		AI182203	
XIX. Translation					
Eif2	3.48	2.70	2.53	AI197161	
Rn18s			3.21	X00686	18SrRNA
Rpl27a		2.66		X05021	L27a
Tceb2		2.09		AA795613	
Eef1d	-2.00			AI836532	
Rps2	-2.00			M20632	
Eif5		-2.00		AW123979	
Rpl13	-2.01			U28917	L13e
Rplp1	-2.02			U29402	LP1
Hnrph1		-2.04		Y14196	
Nxf1	-2.05	-2.10		AF093140	
Eif4g1	-2.06	-2.13		AW380793	
Eif4a2	-2.07	-2.13		X12507	
Hnrpa1		-2.07		AI183202	
Rps28	-2.13			AF110520	S28
Rpl3	-2.16			Y00225	L3
Rps3	-2.17			X76772	S3
Prpf39		-2.17		AI155120	
Arbp	-2.21			X15267	
Rps3a	-2.21			Z83368	S3a
Rps4x	-2.22			M73436	S4
Rpl10	-2.24			M93980	L10
Snrpd3	-2.35			AA796831	L10
Rpl28	-2.36			X74856	L28
Rps8	-2.37			X73829	S8
Rpl10a	-2.39			U12403	L10A
Rpl27a	-2.41			X05021	L27a
Eif2s1	-2.58			AW061243	
Rps7	-2.71			AF043285	S7
Rpl8	-2.87			U67771	L8
Rps16	-2.97			M11408	S16
Eef2	-3.12			M76131	
XX. Misc.					
Emp1			9.56	2.85	X98471
Kdt1	7.93	3.21	2.52	U13371	
Fgl2	5.48	3.29		M16238	
Penk1	5.09			M55181	
Coch	4.80			AF006741	
Wbp5	3.91			U92454	
Crip1		3.79		M13018	
Ect2	3.76	2.57		L11316	
5-Sep	3.63			X61452	
Trim47	3.48			AV077293	
Nr4a2	3.18			U86783	
Cyfip1	3.16	2.19		AF072697	
Dstn		2.97		AB025406	
Nrp		2.89	2.07	D50086	
oaa p.	2.67			M26005	
Bub1	2.65			AI428843	
Stard10		2.49		AW049732	
Bach	2.46	3.34	2.30	AB41279	
Nucb	2.43			M96823	
Rnf138			2.41	AB025011	
Mtv43	2.38	-3.12		M90535	
Cit	2.38			U39904	
Fignl1	2.34	2.10		AI047076	
Clic1		2.32		AF109905	
Spp1	2.31			X13986	
Pon2	2.30			L48514	
Bub1		2.29		AF002823	
Shkbp1	2.24			AV149482	
Rnf138			2.20	AW209763	
Lxn		2.18		D88769	
Klk6	2.15			M13500	
Cpt2	2.15			AV372996	
Tor3a	2.15			AV290846	
Cst7	2.12			AB015224	
Smc2l1		2.11		U42385	
Mcm3	2.09			X62154	
Dp1		2.09		U28168	
Spock2	2.08			AI844853	
Kpna2	2.07	2.19		D55720	
Phf13		2.06		AI605405	
Dnajd1		2.05		AI850983	
Birc5		2.02		AB013819	
Dp1		2.01		AI850356	
Tacc3	2.00	2.58		AW209238	
Gabarapl2		2.00		AI851243	
Wdr13	-2.00			AI850378	
Ftl1	-2.00			L39879	
Akap8	-2.00			AI646981	
Numb	-2.01			U70674	
Ubp1	-2.01			AI836100	
Morf4l2		-2.01		AA529583	
H2-Ke6	-2.02			AF100956	
Etnk1	-2.02			AI853226	
Ascc1	-2.02			AW211207	
Cct4	-2.03			L25913	
Ddx5	-2.02			X65627	
Ddx3x		-2.07		L25126	
Supt5h	-2.03			U88539	
Rpn2	-2.04			D31717	
Dnajb10		-2.04		AI843164	
Bzw2		-2.04		AW060951	
Rap1gds1	-2.06			AW124597	
Cct5	-2.06			Z31555	
Hspa8	-2.08			X54401	
GNAS	-2.09			AW048640	
Ttc3	-2.10	-2.72		AB008516	
Trim28	-2.13			X99644	
Osbpl11	-2.14			AW124363	
Srpk1	-2.15			AB012290	
Bat1a	-2.16			AF118128	
Igfbp4		-2.16	-2.11	X76066	
Npc2	-2.19			AB021289	
Supt4h	-2.19			U96810	
Rere	-2.22	-2.03		AW122831	
Prdx6	-2.22			AF093857	
Fratl2	-2.22			AI846638	
Cxxc5	-2.22	-2.62	-2.81	AW124069	
Rnpc1	-2.23			X75316	
Nrip1		-2.23		AF053062	
Pscdbp	-2.25			AI120844	
Ss18	-2.26			X93357	
Kpnb1	-2.27			D45836	
Cct6	-2.27			Z37164	
Supt4h	-2.30			U96810	
Eng	-2.30			X77952	
Phr1		-2.30		AI836915	
Siah1a	-2.34			Z19579	
Nsun2	-2.35			AI787627	
Cct3	-2.35			L20509	
5830431A10	-2.36			AA168476	
Add1	-2.38			AW121844	
Acp5	-2.38			M90654	
Jmjd1a	-2.39			AW049513	
Gm2a	-2.43			U09816	
Abcn2		-2.43		AV276058	
Rab3ip		-2.54	-2.19	AA798971	
D3Ertd789e			-2.55	AA673252	
Spnb2	-2.58			M74773	
Pdlim1	-2.60			AF053367	
Ppie	-2.64			X68193	
Lef1	-2.70	-2.65	-2.02	D16503	
Ets1	-2.70			AI882555	
Pkp4		-2.80		AI837021	
Xlr3a	-2.82	-2.14		L22977	
Dnajc7	-2.85	-2.46		AI835917	
Gsn	-2.87		-3.76	J04953	
Ilvbl	-2.87			AI842668	
Plac8	-2.89			AA790307	
AW550801	-2.92	-3.40		AI840579	
Rnu22		-2.94		AA684508	
Sfmbt2	-3.02	-3.16	-3.19	AA407367	
D10Wsu52e	-3.02			AI842208	
Smc4l1			-3.02	AA032310	
Ramp1			-3.06	AJ250489	
Phemx			-3.32	AW208513	
Evl	-3.73	-2.89		U72519	
Nsg2	-4.03	-5.38		U17259	
Iap	-4.41			M10062	
Sesn1	-5.05	-4.41	-2.52	AI843106	
Cnn3	-5.05	-5.92	-6.49	AW125626	
Iap11-1	-6.49			X04120	
Erdr1	-6.94	-2.37		AJ007909	

identified in the current analysis as one of the most overexpressed inhibitory receptors by exhausted CD8$^+$ T cells (Table 1 and Tables S2 and S3) consistent with our previous studies (Barber et al., 2006). CTLA-4 mRNA was also overexpressed by exhausted CD8$^+$ T cells, but it is worth pointing out that blockade of CTLA-4 during chronic LCMV infection had little impact on viral load or CD8$^+$ T cell responses (Barber et al., 2006). It is interesting that the inhibitory molecule BTLA (Watanabe et al., 2003) did not appear to be upregulated by exhausted CD8$^+$ T cells (Table S5). Thus, within the CD28:CTLA-4 family there appears to be selective expression or utilization of inhibitory receptors on CD8$^+$ T cells during chronic viral infection.

Many of these molecules contain immunotyrosine inhibitory motifs ITIM, immunotyrosine switch motifs (ITSMs), or both, that can deliver negative signals. For others, the mechanism of signaling is less clear and, in some cases, the available data are conflicting on whether the receptor is activating or inhibitory (e.g., CD160 and 2B4). Of the inhibitory receptors identified by gene-expression profiling, all but two, KLRG1 and KLRA9, are strongly biased or uniquely expressed by exhausted CD8$^+$ T cells

compared to effector and memory CD8$^+$ T cells. It will be important to determine whether these inhibitory receptors impact specific and distinct CD8$^+$ T cell functions or to what extent the inhibitory signals from the pathways might overlap.

Changes in Signaling Potential during Exhaustion

Several genes-encoding key signaling molecules were also differentially expressed by exhausted CD8$^+$ T cells. Lck and NFATc were transcriptionally downregulated in exhausted CD8$^+$ T cells, whereas Fyn was upregulated in both exhausted and effector CD8$^+$ T cells (Table 1 and Tables S2 and S3). In addition, Dgkα was downregulated, whereas the related Dgkγ was upregulated (Table 1 and Tables S2, S3, and S5). Genes involved in calcium binding (up: s100a6, s100a4, s100a11, and s100a13) and Map kinase signaling (up: Map3k4; down: Map4k4 and Mapk8) were also modulated in exhausted CD8$^+$ T cells. The phosphatase Shp1 was transcriptionally reduced in exhausted CD8$^+$ T cells, and this observation might be relevant for the function of some inhibitory receptors or attenuation of TCR signaling.

A number of genes involved in cytokine signaling were also altered in exhausted CD8$^+$ T cells. Cytokine receptor transcripts were altered including both chains of the TNFR (p55 and p75), the IL-4Rα (CD124), and IL-17R. When compared directly to effector or memory CD8$^+$ T cells, IL-18R1 was also downregulated in exhausted CD8$^+$ T cells as were signaling components of the IL-18 and IL-6 receptors pathways (IL-18Rap and IL-6st). It is also worth noting that IL-10 and IL-10R1 mRNA expression was not different among effector, memory, and exhausted CD8$^+$ T cells (data not shown).

A major defect in CD8$^+$ T cells during chronic viral infections is the failure to develop self-renewal and optimal responsiveness to the homeostatic cytokines IL-7 and IL-15 (Shin and Wherry, 2007). Previous studies demonstrated a defect in expression of IL-7 and IL-15 receptors during chronic viral infections, but it was unclear whether receptor expression was the only deficiency in IL-7 and IL-15 responsiveness in these virus-specific CD8$^+$ T cells. IL-7, IL-15, and other gamma-chain cytokine signals in T cells are mediated predominantly by the kinases Jak1, Jak3, and Stat5. The gene-expression profiles of exhausted CD8$^+$ T cells confirmed the low expression of CD127 during exhaustion (Table 1 and Table S3) but also indicated that the deficiencies in cytokine signaling are probably not confined to expression of cell-surface receptors. Although Jak3 message was increased in exhausted CD8$^+$ T cells compared to effector or memory CD8$^+$ T cells (Tables S2 and S3), both Jak1 and Stat5b transcription were reduced (Tables S2 and S5). Indeed, we have recently found that virus-specific CD8$^+$ T cells generated during chronic infection are dependent on viral antigen rather than IL-7 and IL-15 for persistence (Shin et al., 2007). The observations from the gene-expression profiles might provide additional insights into the mechanism behind the poor responsiveness of virus-specific CD8$^+$ T cells to IL-7 and IL-15 during chronic viral infections. These data suggest that CD8$^+$ T cell exhaustion is accompanied by perturbations in the signaling apparatus available to communicate extracellular information via both the TCR and cytokine receptors to the nucleus.

Effector Function

Exhausted CD8$^+$ T cells have a severe defect in cytokine production including IFN-γ (see Figure 1). It was, therefore somewhat surprising that exhausted CD8$^+$ T cells continued to express IFN-γ mRNA in amounts that were intermediate between effector and memory CD8$^+$ T cells (Table 1). Exhausted CD8$^+$ T cells are also poorly cytotoxic ex vivo (Wherry et al., 2003; Zajac et al., 1998), but granzyme B mRNA remains expressed by exhausted CD8$^+$ T cells (Table 1). Perforin mRNA is upregulated in effector and memory CD8$^+$ T cells compared to naive CD8$^+$ T cells, but not in exhausted CD8$^+$ T cells (Table 1). This observation suggests that a deficiency in perforin expression could underlie poor ex vivo cytotoxicity by exhausted CD8$^+$ T cells. In addition, the expression of several genes involved in vesicle transport (down: Snx4, Snx10, and Rabac1) and/or regulation of cytoskeleton (down: Tubb5, Actn1, Macf1, and Actb) was altered in exhausted CD8$^+$ T cells (Table 1 and Tables S2 and S3). It is possible that changes in vesicle trafficking or cytoskeletal rearrangements impact the generation or release of properly formed lytic granules. In contrast, FasL mRNA expression was substantially elevated by exhausted CD8$^+$ T cells compared to naive, effector, and memory CD8$^+$ T cells, and this pathway might provide an alternate cytolytic mechanism during chronic infection. Together, however, poor IFN-γ production and cytotoxicity by exhausted CD8$^+$ T cells cannot be solely attributed to lack of IFN-γ or granzyme B gene expression.

Chemokines and Migration

Exhausted CD8$^+$ T cells displayed upregulation of several chemokine genes including Ccl3 (Mip1α), Ccl4 (Mip1β), and Cxcl10 (IP-10) compared to effector and memory T cells. Ccl5 (Rantes) expression was similar in exhausted and memory CD8$^+$ T cells, both of which expressed slightly lower amounts of this mRNA compared to effector cells. Thus, even in the absence of robust effector function, exhausted CD8$^+$ T cells might retain the ability to "sound the alarm" in an attempt to recruit more effective antiviral T cells to the sites of active viral replication. Future studies will be necessary for determining the importance of these elevated chemokine mRNA levels in the in vivo response of exhausted CD8$^+$ T cells.

Exhausted CD8$^+$ T cells also have altered expression of molecules involved in cell adhesion (up: Itgax [CD11c], neuropilin, Itga4 [CD49d], Itgb1 [CD29], CD166, Itgb2 [CD18], and ItgaV [CD51]; down: Icam2, Itgae, Sema4a, and Itgb7) and migration and chemotaxis (up: Ccr5, Cxcr3, Ccrl2; down: Edg6, Ccr7, CD62L), suggesting possible changes in migratory properties in vivo. Indeed, several studies have documented altered tissue distribution of virus-specific CD8$^+$ T cells during chronic infections (He et al., 1999; Wherry et al., 2003).

Transcription Factors in CD8+ T Cell Exhaustion

Transcription factors and genes involved in transcriptional regulation was another group of mRNAs substantially altered by exhausted CD8+ T cells. This set of genes included at least 15 mRNAs that were uniquely or selectively upregulated and 11 that were dowregulated in exhausted CD8+ T cells. These observations are consistent with the notion that exhausted CD8+ T cells arise from an altered pattern of differentiation compared to functional effector and memory T cells.

PBX3 was the most differentially expressed transcription factor in exhausted CD8+ T cells (Table 1 and Tables S2 and S3). PBX3 is a TALE class homeodomain transcription factor implicated in developmental regulation (Sagerstrom, 2004), but the role of PBX3 in CD8+ T cell differentiation has not been explored.

A second transcription factor that was of considerable interest and that was revealed by the gene-expression profiles is Blimp-1 (Prdm1). The increased expression of Blimp-1 in virus-specific effector and exhausted CD8+ T cells is intriguing, given the role of this transcription factor in regulating terminal differentiation in germinal center B cells (Calame, 2006). Recent studies have revealed an important role for Blimp-1 in regulating T cell responses (Kallies et al., 2006; Martins et al., 2006), but precisely how this transcriptional repressor controls T cell differentiation remains unclear. It will be of considerable interest to investigate how Blimp-1 regulates virus-specific CD8+ T cell differentiation during chronic viral infection.

Several additional transcription factors were also revealed by the gene-expression profiles of exhausted CD8+ T cells including several upregulated (e.g., Eomes, NFaTc1, Jak3, nurr1, and Maf) and downregulated (e.g., Fos, Fosb, junb, myb, and Myc) molecules of potential immunological interest. Eomes is of note given the influence of this molecule on the transcriptional regulation of effector genes (e.g., granzyme B and IFN-γ) and cd122 (Intlekofer et al., 2005; Pearce et al., 2003). Several Klf family members are also downregulated in exhausted CD8+ T cells including Klf2, Klf3, Klf4, and Klf13. In particular, changes in Klf2 expression might be important in the exhausted CD8+ T cells because Klf2 can regulate T cell quiescence and migration (Carlson et al., 2006; Kuo et al., 1997). Together, these findings show that the expression of genes involved in regulating transcription in exhausted CD8+ T cells highlights the altered pattern of differentiation in these T cells.

Metabolic Defects in Exhausted CD8+ T Cells

Metabolic and bioenergetic deficiencies in exhausted CD8+ T cells were among the most striking patterns that emerged from the gene-expression profiles. A large number of ribosomal subunits were transcriptionally downregulated in exhausted CD8+ T cells compared to naive, effector, and memory T cells (Table 1 and Tables S2, S3, and S5). Up to 17 ribosomal subunits, three elongation factors, and four initiation factors were downregulated in exhausted CD8+ T cells.

In addition to translational defects, the gene-expression profiles also suggest other fundamental metabolic and bioenergetic changes during CD8+ T cell exhaustion. For example, a number of genes involved in energy metabolism and the citric-acid cycle were transcriptionally downregulated in exhausted CD8+ T cells but not effector or memory CD8+ T cells including Acas2l, Sdha, Adcy7, Pdha1, and Acadm. Other metabolic pathways transcriptionally altered in exhausted CD8+ T cells included solute and ion channels and aquaporins (Table 1 and Tables S2, S3, and S5). These observations suggest that bioenergetic deficiencies in exhausted CD8+ T cells might impact functional responsiveness and perhaps the long-term fitness and survival of this CD8+ T cell population.

Other Genes and Pathways of Interest

Several other major classes of mRNAs were altered in exhausted CD8+ T cells. These include changes in expression of genes involved in glycosylation, increases in IFN-responsive genes, and several protease mRNAs including upregulation of serpins, some of which can protect from T cell-mediated cytotoxicity (Liu et al., 2004). Several caspases (1, 3, and 4) were upregulated, and Bcl-2 family members were upregulated and downregulated. The precise balance of these proapoptotic and antiapoptotic molecules is difficult to infer simply from the mRNA-expression profiles. However, the mRNA profiles suggest that the regulation of apoptosis is likely to be quite different in the exhausted CD8+ T cells compared to naive, effector, and memory CD8+ T cells. Many cell-cycle genes were changed in exhausted CD8+ T cells, and these changes are predominantly consistent with increased expression of checkpoint proteins and reduced expression of prodivision signals.

Several specific genes are also worth noting simply on the basis of their expression profile including plekstrin (up ~35- and ~60-fold in exhausted and effector CD8+ T cells), Folate receptor 4 (up in exhausted), and Tmem2 (up in exhausted) (Table 1 and Table S5). Finally, KLRG1 was the most effector-biased gene when exhausted and effector CD8+ T cells were directly compared to each other (Table S2).

Progression of CD8+ T Cell Dysfunction during Exhaustion

It was of interest to understand how CD8+ T cell exhaustion and the expression of markers of T cell differentiation change during the course of chronic infection and development of exhaustion. To address this issue, we performed a kinetic analysis of both functional exhaustion and phenotypic differentiation of virus-specific CD8+ T cells after infection with either Arm or clone 13. At day 6 p.i. GP33-specific CD8+ T cells in both Arm- and clone 13-infected mice were functional, and a similar proportion of tetramer+ CD8+ T cells was capable of producing IFN-γ during both infections (Figures 3A and 3B). Although there were slightly fewer IFN-γ and TNF-α coproducers during clone 13 infection at day 6, the amount of IFN-γ, TNF-α, and IL-2 produced (MFI) by the virus-specific CD8+ T cells

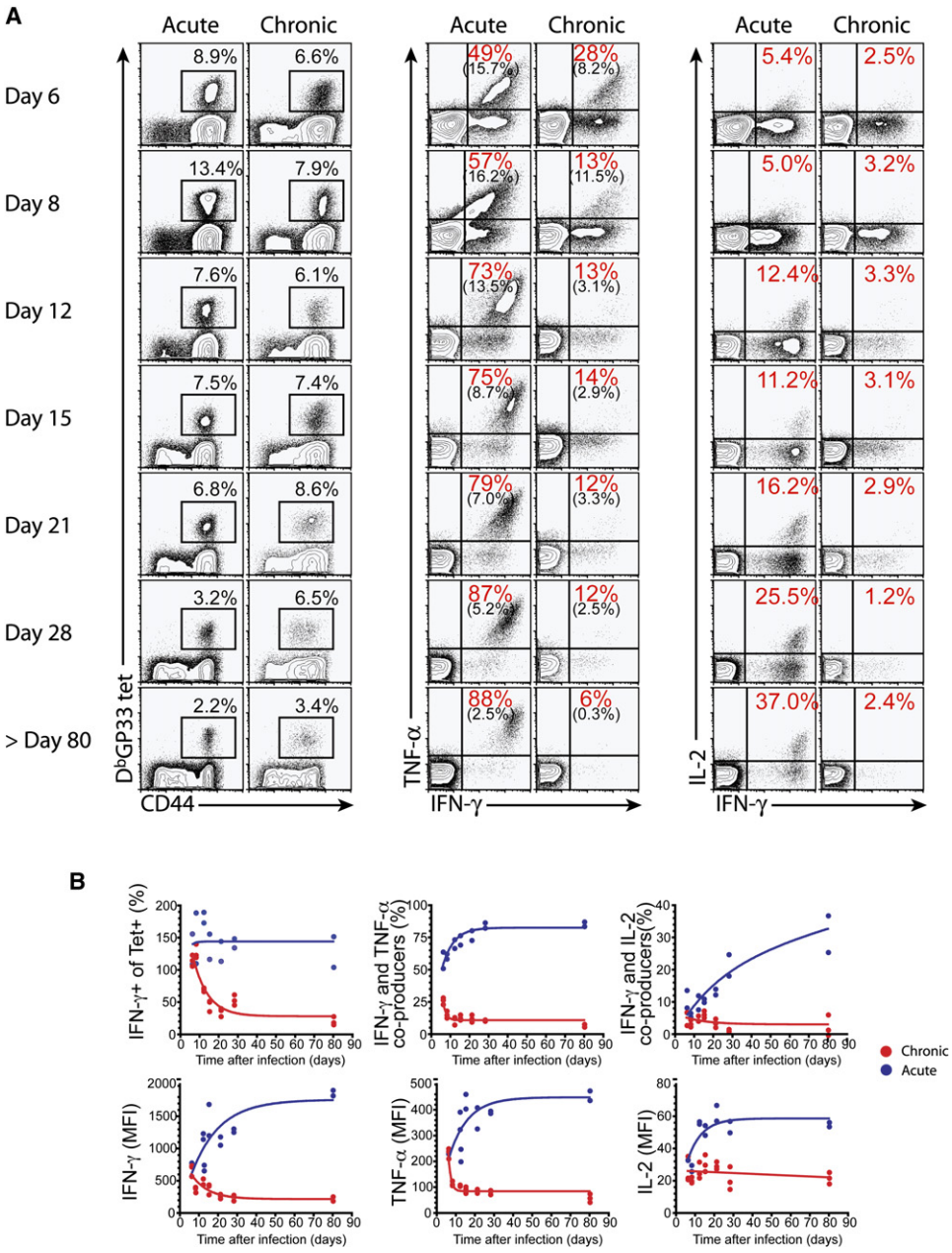

Figure 3. Kinetics of Exhaustion during Acute versus Chronic LCMV Infection: Functional Exhaustion

(A) LCMV DbGP33-specific CD8$^+$ T cells were identified by tetramer staining in the spleen at the indicated times p.i. with Arm versus clone 13 (left panels). Numbers represent the percent of tetramer$^+$ of CD8$^+$ T cells. Samples from the same mice were also stimulated with GP33 peptide and IFN-γ, TNF-α, and IL-2 assessed by ICS (IFN-γ + TNF-α coproduction, middle panel; IFN-γ + IL-2 coproduction, right panel). The percentage in red is the percentage of cytokine coproducers out of the total IFN-γ$^+$ population. The percentage in parentheses indicates the total percent of CD8$^+$ T cells producing IFN-γ (middle panels).

(B) The percent of tetramer$^+$ cells capable of making IFN-γ is shown in the upper left panel. The upper middle and upper right panels indicate the percentage of IFN-γ + TNF-α and IFN-γ + IL-2 coproducers at various times p.i. The bottom panels display the MFI for IFN-γ (left), TNF-α (middle), and IL-2 (right). All responses are for GP33-specific CD8$^+$ T cells. Data represents two to six independent experiments depending on the time point.

after either infection was very similar (Figure 3B). Over the ensuing weeks after clearance of infection, virus-specific CD8$^+$ T cells generated during acute infection all remained functional (all tetramer$^+$ cells produced IFN-γ), and in fact, the percentage cells coproducing multiple cytokines (IFN-γ + TNF-α and IFN-γ + IL-2 coproducers) and the amount of cytokine produced per cell (MFI) increased. In contrast, during chronic LCMV infection, virus-specific CD8$^+$ T cells became progressively less functional over time. By 2–3 weeks p.i., 50% or more of the tetramer$^+$ cells could not

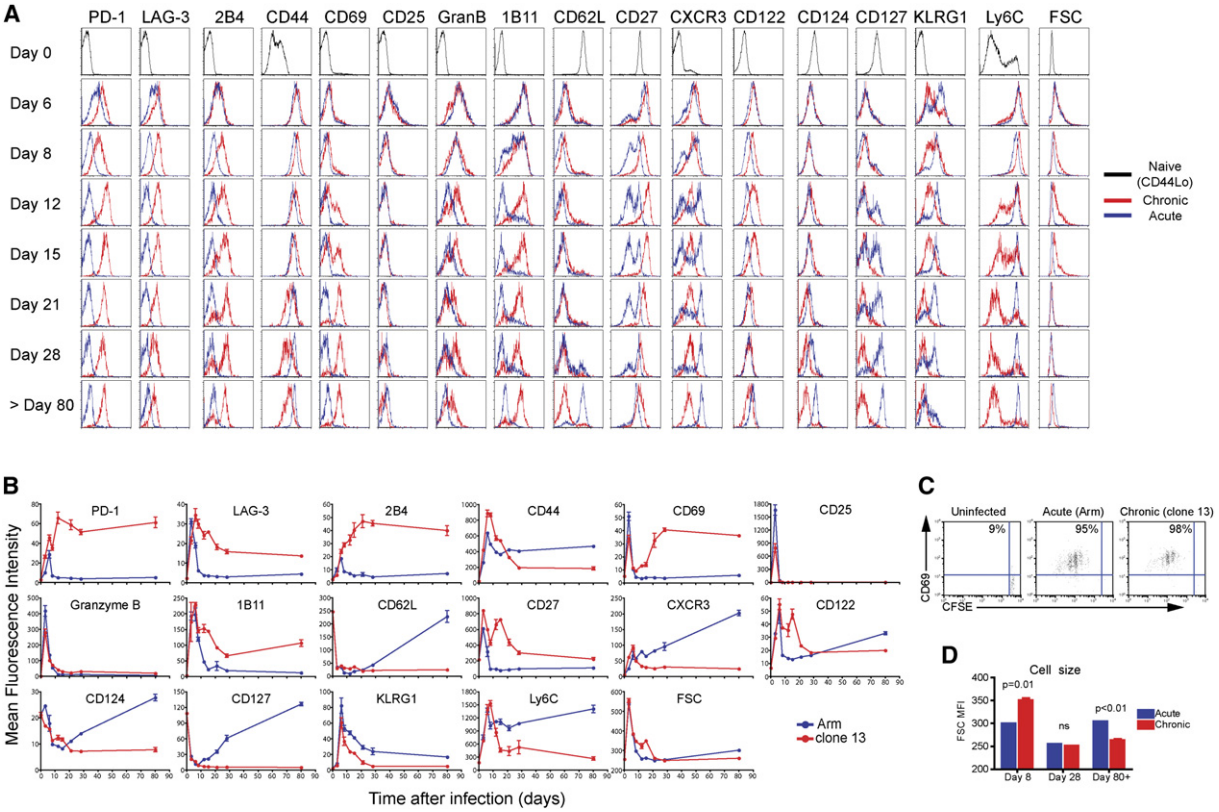

Figure 4. Kinetics of Exhaustion during Acute versus Chronic LCMV Infection: Phenotypic Differentiation

(A) The expression of the indicated molecules was assessed over time on DbGP33 tetramer$^+$ CD8$^+$ T cells after Arm (blue histograms) or clone 13 (red histograms) infection. All plots are gated on CD8$^+$DbGP33$^+$ except the top row, which is gated on CD8$^+$CD44^{Lo} cells.

(B) A summary of the kinetic analysis in (A) is shown for each marker at multiple time points after Arm (acute infection; blue lines) or clone 13 (chronic infection; red lines).

(C) Naive CFSE-labeled DbGP33-specific P14 cells were adoptively transferred to naive mice, and these mice were either left uninfected or infected with LCMV Arm or clone 13. Three days later, CD69 expression and division of the donor P14 cells was assessed by flow cytometry.

(D) The MFI of FSC for DbGP33 tetramer$^+$ CD8$^+$ T cells is summarized for acute versus chronic infection (n = 2–3 per group). Data represents two to six independent experiments depending on the time point. Error bars indicate SD, and p values were determined by t test.

produce IFN-γ, and the frequency of cytokine coproducers and amount (MFI) of individual cytokines produced per cell declined dramatically (Figure 3B). Thus, although virus-specific CD8$^+$ T cells were initially functional after both Arm and clone 13 infections, during chronic LCMV infection, virus-specific CD8$^+$ T cells become progressively less functional (i.e., exhausted) after the first week of infection.

Altered T Cell Differentiation during Exhaustion

We next profiled the phenotypic changes in virus-specific CD8$^+$ T cells during the progression to exhaustion versus development of memory by using a set of genes identified by microarray analysis. At day 6 p.i., the inhibitory receptors PD-1, LAG-3, and 2B4 were upregulated on DbGP33-specific CD8$^+$ T cells during both Arm and clone 13 infection (PD-1 was perhaps slightly higher during clone 13 infection at this time point.). However, by day 8 p.i., the expression of these inhibitory receptors was low during Arm infection and remained low thereafter, consistent with the clearance of the virus. In contrast, during chronic infection, PD-1, LAG-3, and 2B4 remained highly expressed, and especially for PD-1 and 2B4, the expression increased on virus-specific CD8$^+$ T cells after day 8 (Figures 4A and 4B). Thus, expression of inhibitory receptors is not unique to chronic viral infection. Rather, during initial T cell activation during both acute and chronic infection, these pathways are upregulated; yet, at these early time points, T cells are functional. It is possible that early during infection signals from positive costimulatory pathways outweigh those from negative pathways. Later, during chronic infection, the persistent (and increased) expression of inhibitory receptors might shift the balance toward inhibition of T cell function. Future studies will be necessary for determining precisely when and how these inhibitory pathways control antiviral T cell function in vivo.

At early times p.i. (day 6), virus-specific CD8$^+$ T cells primed during acute versus chronic infection expressed a similar pattern of activation and differentiation markers including CD44, CD25, granzyme B, 1B11, CD62L, CD27,

CXCR3, and Ly6C. In contrast to acute infection, however, virus-specific $CD8^+$ T cell expression of granzyme B and 1B11 remained elevated during chronic infection, whereas CD62L remained low. The activation marker CD69 was low at day 6 (Figure 4C) after both Arm and clone 13 infection despite the presence of antigen. To examine whether CD69 was expressed earlier during infection, we used a P14 adoptive transfer approach to visualize virus-specific $CD8^+$ T cells at day 3 p.i. At this time point, CD69 expression was elevated after both Arm and clone 13 infections, and a similar profile of CD69 expression versus cellular division was observed (Figure 4C). During clone 13 infection, CD69 again began to increase after day 12 and was uniformly high on virus-specific $CD8^+$ T cells from chronically infected mice after day 21. The reasons for this dynamic regulation of CD69 are not clear but suggest that there might be a period of time early during infection when T cells are refractory to further upregulation of CD69.

Although CD44 expression was elevated compared to naive $CD8^+$ T cells after both infections, beginning ~3 weeks p.i., CD44 expression was lower on exhausted $CD8^+$ T cells compared to memory $CD8^+$ T cells consistent with the microarray data (Table S5). CD27 is of interest because this molecule has been used extensively to characterize human antiviral $CD8^+$ T cells responding to different persisting infections (van Lier et al., 2003). Although two subsets of antiviral $CD8^+$ T cells were clearly present on the basis of CD27 expression during the first ~3-4 weeks after acute infection, only $CD27^{hi}$ cells were found during chronic infection. Memory $CD8^+$ T cells also eventually all became $CD27^{hi}$. Other molecules including CXCR3 and Ly6C also displayed dynamic expression patterns that differed between the development of memory ($CXCR3^{hi}Ly6C^{hi}$) and exhausted ($CXCR3^{int}Ly6C^{lo}$) $CD8^+$ T cells.

The expression of the cytokine receptors CD122, CD124, and CD127 was low on exhausted $CD8^+$ T cells at late time points during chronic infection compared to memory $CD8^+$ T cells. CD124 and CD127 were permanently downregulated early after infection in contrast to the re-expression of these cytokine receptors after acute infection (Figure 4C and Figure S2). CD122, on the other hand, was similar after acute or chronic infection at day 6, was higher on exhausted $CD8^+$ T cells from day 8 to day 21, but eventually became lower in exhausted compared to memory $CD8^+$ T cells at later times p.i. The expression pattern of these receptors is consistent with the gene-expression data (Table 1 and Tables S2, S3, and S5) and suggests that exhausted $CD8^+$ T cells will not efficiently respond to IL-2, IL-4, IL-7, and IL-15 at later times p.i.

KLRG1 was one of the few molecules examined that differed in protein expression at early time points after infection. During clone 13 infection, virus-specific $CD8^+$ T cells expressed lower amounts of KLRG1 at day 6 (and at all subsequent time points) compared to virus-specific $CD8^+$ T cells generated after Arm infection. Expression of KLRG1 by $CD8^+$ T cells has been associated with repetitive antigen stimulation, cellular senescence, and terminal differentiation (Joshi et al., 2007; Masopust et al., 2006; Voehringer et al., 2001). The $KLRG1^{lo}$ phenotype of exhausted $CD8^+$ T cells was, therefore, a bit surprising because these cells have a poor proliferative capacity upon antigen stimulation (Wherry et al., 2004; Wherry et al., 2005). It will be interesting to determine how the relationship between KLRGI expression and proliferative potential applies to chronic infection during which the T cells experience continuous rather than intermittent antigen stimulation.

Finally, virus-specific $CD8^+$ T cells were larger in size during chronic infection compared to after acute infection between days 8-15. This difference likely reflects persisting TCR stimulation during clone 13 infection, but not following Arm infection at these time points. However, exhausted $CD8^+$ T cells were significantly smaller than memory $CD8^+$ T cells at later time points (Figures 4A, 4B, and 4D). This reduced cell size for exhausted $CD8^+$ T cells is one of the last differences to emerge. Cell size is an excellent indicator of metabolic fitness, and when metabolism is compromised, lymphocytes become considerably smaller (Rathmell et al., 2000). The observations on the size of exhausted compared to memory $CD8^+$ T cells are in good agreement with the gene-expression profile of metabolic fitness described above.

Gene-Expression Profile of Exhaustion Is Distinct from Anergy

Exhaustion of antigen-specific $CD8^+$ T cells has been described during a number of both experimental and human infections. Anergy also results in T cell dysfunction. Anergy occurs when initial TCR signals are received in the absence of optimal costimulation leading to a state of hyporesponsiveness (Schwartz, 2003). A transcriptional signature of anergy has been defined, resulting in the identification of 14 anergy-associated genes (Macian et al., 2002). In this study, anergized T cells were refractory to subsequent anti-CD3 stimulation and had decreased transcription of several cytokine genes including *Il2*, *Ifng*, *Tnf*, and *Ccl3*. The expression profile of anergy-associated genes was also examined with an in vivo tolerance model in which many of the anergy-associated genes identified in vitro were confirmed, thus defining a molecular signature of anergy both in vitro and in vivo (Macian et al., 2002).

To examine whether exhaustion and anergy shared similar transcriptional signatures, we examined the expression pattern of the 14 anergy associated genes identified by Macian et al. (2002) in the exhausted $CD8^+$ T cells. Few of the anergy-associated genes were upregulated in exhausted $CD8^+$ T cells (Figure 5A). Also, this panel of 14 genes did not clearly distinguish exhausted $CD8^+$ T cells from effector or memory $CD8^+$ T cells. In this type of analysis, the expression of individual anergy-associated genes was assessed relative to a threshold value (i.e., ±2-fold). It remained possible that, although the anergy-associated genes were not individually overexpressed >2-fold in exhausted $CD8^+$ T cells, these genes as a set might be specifically enriched during exhaustion. To test this possibility, we next used gene-set-enrichment

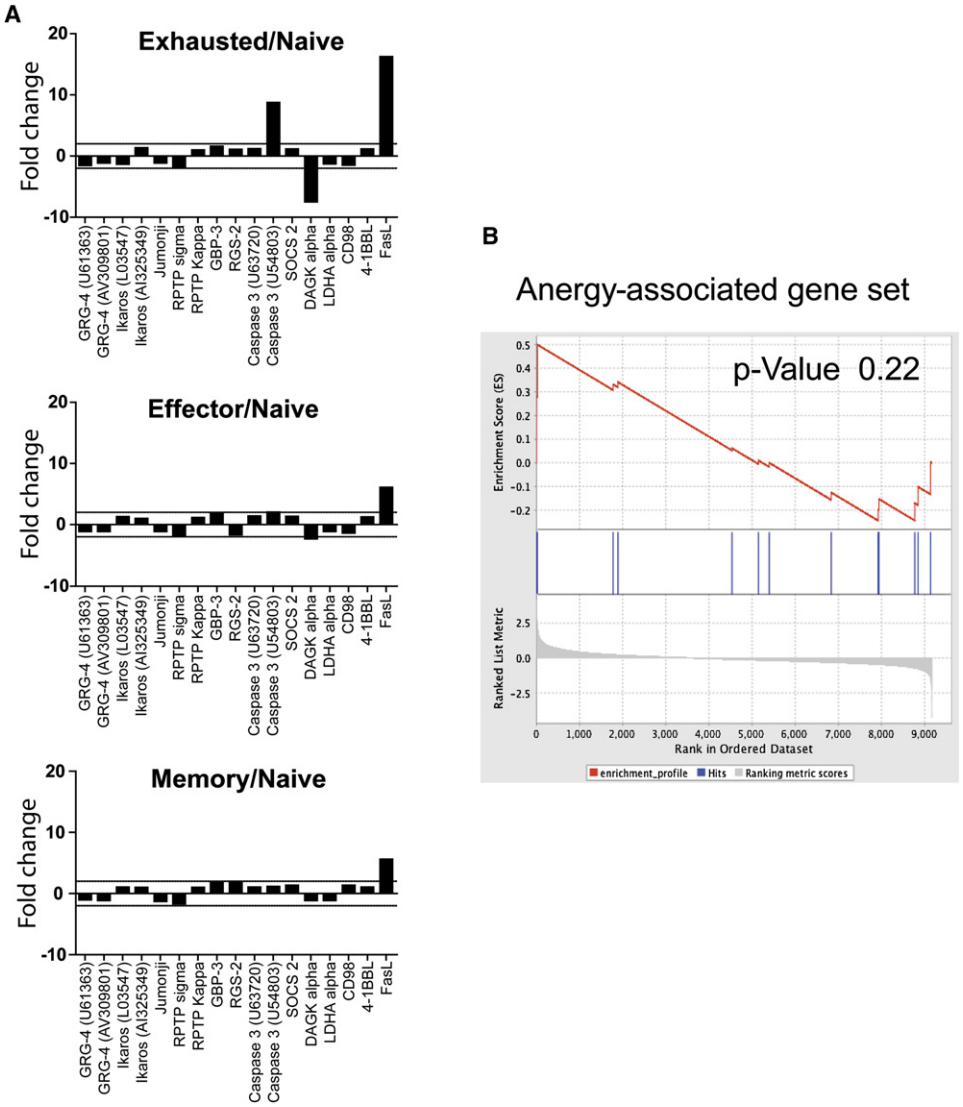

Figure 5. Gene-Expression Profiles of Exhaustion Are Distinct from Anergy

(A) The expression of 14 anergy-associated genes was determined for the exhausted, effector, and memory profiles with the U74A gene-expression data.

(B) We performed gene-set-enrichment analysis (GSEA) to determine whether the anergy-associated gene set showed specific enrichment in the exhausted $CD8^+$ T cells. The p value for specific enrichment of the gene set is indicated.

analysis (GSEA; [Subramanian et al., 2005]) (Figure 5B). GSEA is performed by assigning a rank order to the expression of the ~9000 genes from the U74A arrays (ESTs are excluded from this analysis.). The location of each gene of interest is then determined in the rank-ordered data set, and the specific enrichment of the set of genes at the higher (or lower) ends of the rank order is determined. As shown in Figure 5B, the anergy-associated gene set did not show specific enrichment in the exhausted $CD8^+$ T cells, and the "hits" for the individual genes were distributed essentially throughout the rank order and not accumulated on the left side as is expected for enriched genes (Subramanian et al., 2005). Taken together, the data in Figure 5 suggest that $CD8^+$ T cell exhaustion examined in the current study is distinct from the process of anergy profiled in previous studies (Macian et al., 2002). Thus, T cell exhaustion and anergy, at least for these two models, do not appear to share the same transcriptional signature.

DISCUSSION

A number of pathways, identified in the present study, are associated with $CD8^+$ T cell exhaustion during chronic viral infection. One of the most obvious patterns that emerged was the overexpression of cell-surface inhibitory molecules by virus-specific $CD8^+$ T cells during chronic infection. Our previous observations on the role of PD-1

in regulating exhaustion (Barber et al., 2006) suggest that the group of inhibitory pathways identified in the current study might provide additional targets for investigation. It will be important to determine whether inhibitory pathways such as LAG-3, 2B4, and GP49B have distinct or overlapping roles in regulating T cell responses during chronic infection. A puzzling issue is why exhausted $CD8^+$ T cells would express multiple receptors with inhibitory function. One possibility is that these are redundant pathways for ensuring adequate control of immunopathology. A second possibility is that these different receptors have nonoverlapping intracellular signaling targets. A third possibility is that the expression of the ligands for these receptors is a key to their effective inhibition of T cell responses. The ligands for the inhibitory receptors overexpressed by exhausted $CD8^+$ T cells include a diverse array of both cell-surface and soluble molecules expressed in a restricted (e.g., professional APC only) or broadly distributed manner. A combination of these mechanisms might explain the apparent redundancy of inhibitory receptors. Future studies are aimed at investigating the roles of these different pathways in regulating $CD8^+$ T cells during chronic viral infections.

A second novel observation revealed by the transcriptional profiles of exhausted $CD8^+$ T cells was the dramatic alteration in metabolic and bioenergetic pathways compared to the pathways of naive, effector, and memory T cells. Exhausted $CD8^+$ T cells downregulated components of the translational machinery, molecules involved in the citric-acid cycle, and energy metabolism, and these cells also became considerably smaller in size. One implication of downregulated ribosomal subunits is that these cells might have difficulty producing the quantity of cytokines or other effector proteins normally produced by functional effector and memory $CD8^+$ T cells. This interpretation would also fit with the predominantly intact expression of the mRNA for such as IFN-γ and granzymes B, A, and K.

Cell size is a useful indicator of metabolic fitness (Rathmell et al., 2000), suggesting that the reduction in cell size for exhausted $CD8^+$ T cells reflects some of the metabolic deficiencies observed in the gene-expression profiles. It is interesting to note that the inhibitory receptors PD-1 and CTLA-4 can impair optimal AKT activation, a key signaling pathway for glucose utilization and cellular metabolism (Parry et al., 2005). Impaired translational machinery and metabolic fitness is also likely to impede robust proliferation. Production of a new complement of cellular proteins and the increase in cell size necessary to give rise to two daughter cells during mitosis might be substantially compromised by the bioenergetic and ribosomal deficiencies present in exhausted $CD8^+$ T cells. It should be noted, however, that these metabolic changes do not universally prevent protein translation because a number of molecules, such as the inhibitory receptors, are upregulated in exhausted $CD8^+$ T cells at the protein level. It will probably be important to address these bioenergetic and translantion deficiencies in therapeutic strategies aimed at restoring optimal function from exhausted T cells.

Kinetic profiling of T cell dysfunction and differentiation during chronic infection confirmed the expression pattern of many proteins predicted by the gene-expression profiles. More importantly, this kinetic analysis demonstrated the progressive nature of $CD8^+$ T cell exhaustion. Of the 22 properties examined by flow cytometry (including cytokine coproduction), only three differed between virus-specific $CD8^+$ T cells from Arm and clone 13 infection at day 6 p.i. (TNF-α + IFN-γ coproduction, PD-1, and KLRG1). By day 8 p.i., nine differences were apparent. After day 8 of acute infection, virus-specific $CD8^+$ T cells continued to progressively differentiate into memory T cells and acquired new phenotypic and functional characteristics such as IL-2 production. T cell exhaustion, in contrast, followed an altered pattern of differentiation, and after day 8 of infection, the differences between functional memory T cell differentiation and exhaustion continued to increase. Between 1–2 weeks p.i., 18 of 22 properties profiled differed, and after $\sim$1 month, this had increased to 20 or 21 differences out of 22 properties examined. Thus, our results indicate that $CD8^+$ T cell exhaustion is a graded process during chronic viral infection and that there are stages in the differentiation and development of exhausted $CD8^+$ T cells. Such a graded or progressive development of $CD8^+$ T cell exhaustion might have implications for therapeutic strategies that could be tailored to overcome specific defects of a particular stage of exhaustion.

Our data also suggest that T cell anergy and exhaustion occur by distinct molecular mechanisms. In addition to the anergy-associated gene set identified by Macian et al. (2002), several other genes have been reported to be associated with T cell anergy including Egr-2, Egr-3 (Harris et al., 2004; Safford et al., 2005), and grail (Mueller, 2004). These genes were not selectively expressed by exhausted $CD8^+$ T cells compared to functional effector and memory $CD8^+$ T cells. Recent evidence suggests that the proper NFAT:AP-1 ratio promotes T cell activation, whereas NFAT activity in the absence of AP-1 favors anergy (Macian et al., 2002). Indeed, NFATc1 is transcriptionally elevated in exhausted $CD8^+$ T cells, and Fos (part of the AP-1 dimer), Fosb, and Junb are downregulated in exhausted $CD8^+$ T cells compared to memory $CD8^+$ T cells. Thus, some alterations in the NFAT:AP-1 balance might exist in exhausted $CD8^+$ T cells compared to memory $CD8^+$ T cells, but the lack of expression of target genes of AP-1-independent NFAT transcription such as E3 ubiquitin ligases (Heissmeyer et al., 2004) suggest that the major transcriptional mechanisms of anergy and exhaustion are predominantly distinct.

Mouse models including LCMV have been invaluable in dissecting T cell responses to chronic viral infections. For example, recent studies on the role of the PD-1 pathway in regulating $CD8^+$ T cell exhaustion first during LCMV, and soon thereafter for HIV, HBV, and HCV infection highlight the translation of observations from mouse models to human viral infection (Barber et al., 2006; Boni et al., 2007; Day et al., 2006; Petrovas et al., 2006; Radziewicz et al., 2006; Trautmann et al., 2006; Urbani et al., 2006). It will be important in the future to determine whether additional

features of the molecular signature of CD8$^+$ T cell exhaustion in the LCMV model can also be extended to humans. Recent studies suggest that the transcriptional profile of HIV-specific CD8$^+$ T cells from humans might indeed share similarities to exhausted LCMV-specific CD8$^+$ T cells (W.N.H. and T.R. Golub, unpublished data). Future studies will be necessary to determine the therapeutic implications of pathways revealed by transcriptional profiling of mouse and human CD8$^+$ T cells responding to chronic viral infections.

In summary, these studies provide a framework with which to begin dissection of the factors that influence virus-specific CD8$^+$ T cell differentiation during chronic infections. In addition, these studies identify a number of inhibitory, signaling, and metabolic pathways that might underlie the functional defects in these CD8$^+$ T cells and might also represent novel targets for immunotherapy.

EXPERIMENTAL PROCEDURES

Mice and Infections

Four- to six-week-old female C57BL/6 mice were purchased from The Jackson Laboratory. We used the LCMV-specific P14 TCR transgenic system to generate effector and memory CD8$^+$ T cells as described (Kaech et al., 2002). In brief, P14 chimeras were made by adoptive transfer of a small number of naive P14 CD8$^+$ T cells ($\sim 5 \times 10^4$) to naive congenic recipient mice followed by LCMV infection. For acute infections, mice were infected with 2×10^5 pfu of LCMV Arm i.p. For chronic infections, mice were given 2×10^6 pfu of LCMV clone 13 i.v. and depleted of CD4$^+$ T cells with 200 μg GK1.5 on days −1 and +1 p.i. Viral titers in chronically infected mice were verified by plaque assay in the serum prior to use. Plaque assays were performed as previously described (Wherry et al., 2003).

Lymphocyte Isolation, Flow Cytometry, and Functional Analysis

Lymphocytes were isolated and MHC class I peptide tetramers were generated and used as previously described (Wherry et al., 2003). All antibodies were obtained from BD Bioscience (San Diego, CA) except for granzyme B and KLRG1 (Caltag). Intracellular cytokine staining was performed as previously described (Wherry et al., 2003). Elisas were performed with kits from R&D systems according to the manufacturer's instructions.

Cell Sorting

Naive LCMV DbGP33-specific P14 T cells isolated directly from naive P14 mice. Effector and memory CD8$^+$ T cells from P14 chimeras were sorted on day 8 or >day 30 after LCMV Arm infection respectively. LCMV-specific CD8$^+$ T cells were sorted on a BD Facs Vantage or Cytomation MoFlo with congenic markers (Thy1.1) for naive, effector, and memory CD8$^+$ T cells as described (Kaech et al., 2002). For technical reasons, it was not possible to use the P14 system during chronic LCMV infection. Exhausted CD8$^+$ T cells (day 22–35 p.i.) were sorted with MHC tetramers (DbGP33 n = 3 and DbGP276 n = 1). All samples were maintained at 4°C for the duration of the sort, and purity was 95%–98% for all populations.

RNA Amplification and Hybridization

Total RNA was isolated from sorted naive, effector, memory, and exhausted CD8$^+$ T cells using Trizol (GIBCO/BRL Life Technologies, Rockville, MD) according to the manufacture's instructions. cDNA was synthesized and amplified as described (Kaech et al., 2002). Samples were hybridized to Affymetrix U74Av2, Bv2, or Cv2 microarrays at Emory University or at the Vanderbilt University Microarray Shared Resource. Three to four samples were hybridized to the U74Av2 microarrays for each cell type, whereas two exhausted, two naïve, and one each for memory and effector were hybridized to U74Bv2 and U74Cv2 arrays. Because of the lower number of samples for the B and C arrays, these data were not included in clustering analyses.

Microarray-Data Analysis

Gene Chip Murine Genome U74Av2 Array was used for the microarray-data-analysis study (see: http://www.affymetrix.com/products/arrays/specific/mgu74.affx).

We performed quality-control checks with R-pack (BioConductor) to verify technical replicates and their quality. Data analysis and clustering was done in gene-chip-analysis software GeneSpring GX 7.3 Agilent (see: http://www.chem.agilent.com/Scripts/PDS.asp?lPage = 27881). The data were preprocessed with RMA (Robust Multichip Average) normalization. There were four technical replicates for each cell type, naive, memory, and exhausted, and three for effectors. Technical replicates were averaged for fold-change study. RMA expression values for genes upregulated and downregulated by 2.0-fold change between each cell types were exported from Genespring to Microsoft Excel and analyzed further. We used K means clustering with Pearson correlation to understand how similar or distant each of the cell types were from one another with respect to naive. RMA expression values with 1.4-fold cutoff between all four cell types were used as input for pathway analysis in Ingenuity pathway analysis software (Ingenuity Systems). GSEA was performed as described (Subramanian et al., 2005).

Supplemental Data

One figure and five tables are available at http://www.immunity.com/cgi/content/full/27/4/670/DC1/.

ACKNOWLEDGMENTS

We thank P. Mahar, S. Jenkins, Y. Blinder, and B. Konieczny for technical assistance and R. Karaffa and M. Hulsey for FACS sorting. This work was supported by the National Institutes of Health (NIH) (grant AI30048 to R.A. and AI071309 to E.J.W.) and the Foundation for NIH and Bill and Melinda Gates foundation (to R.A.), Elizabeth Glaser Pediatric AIDS Foundation Scholar Awards (to S.S. and V.K.), and a Cancer Research Institute postdoctoral fellowship (to E.J.W.).

Received: February 2, 2007
Revised: July 10, 2007
Accepted: September 17, 2007
Published online: October 18, 2007

REFERENCES

Ahmed, R., Salmi, A., Butler, L.D., Chiller, J.M., and Oldstone, M.B. (1984). Selection of genetic variants of lymphocytic choriomeningitis virus in spleens of persistently infected mice. Role in suppression of cytotoxic T lymphocyte response and viral persistence. J. Exp. Med. *160*, 521–540.

Assarsson, E., Kambayashi, T., Persson, C.M., Chambers, B.J., and Ljunggren, H.G. (2005). 2B4/CD48-mediated regulation of lymphocyte activation and function. J. Immunol. *175*, 2045–2049.

Barber, D.L., Wherry, E.J., Masopust, D., Zhu, B., Allison, J.P., Sharpe, A.H., Freeman, G.J., and Ahmed, R. (2006). Restoring function in exhausted CD8 T cells during chronic viral infection. Nature *439*, 682–687.

Boni, C., Fisicaro, P., Valdatta, C., Amadei, B., Di Vincenzo, P., Giuberti, T., Laccabue, D., Zerbini, A., Cavalli, A., Missale, G., et al. (2007). Characterization of hepatitis B virus (HBV)-specific T-cell dysfunction in chronic HBV infection. J. Virol. *81*, 4215–4225.

Brooks, D.G., Trifilo, M.J., Edelmann, K.H., Teyton, L., McGavern, D.B., and Oldstone, M.B. (2006). Interleukin-10 determines viral clearance or persistence in vivo. Nat. Med. *12*, 1301–1309.

Calame, K. (2006). Transcription factors that regulate memory in humoral responses. Immunol. Rev. *211*, 269–279.

Carlson, C.M., Endrizzi, B.T., Wu, J., Ding, X., Weinreich, M.A., Walsh, E.R., Wani, M.A., Lingrel, J.B., Hogquist, K.A., and Jameson, S.C. (2006). Kruppel-like factor 2 regulates thymocyte and T-cell migration. Nature *442*, 299–302.

Day, C.L., Kaufmann, D.E., Kiepiela, P., Brown, J.A., Moodley, E.S., Reddy, S., Mackey, E.W., Miller, J.D., Leslie, A.J., Depierres, C., et al. (2006). PD-1 expression on HIV-specific T cells is associated with T-cell exhaustion and disease progression. Nature *443*, 350–354.

Ejrnaes, M., Filippi, C.M., Martinic, M.M., Ling, E.M., Togher, L.M., Crotty, S., and von Herrath, M.G. (2006). Resolution of a chronic viral infection after interleukin-10 receptor blockade. J. Exp. Med. *203*, 2461–2472.

Fuller, M.J., and Zajac, A.J. (2003). Ablation of CD8 and CD4 T cell responses by high viral loads. J. Immunol. *170*, 477–486.

Greenwald, R.J., Freeman, G.J., and Sharpe, A.H. (2005). The B7 family revisited. Annu. Rev. Immunol. *23*, 515–548.

Harris, J.E., Bishop, K.D., Phillips, N.E., Mordes, J.P., Greiner, D.L., Rossini, A.A., and Czech, M.P. (2004). Early growth response gene-2, a zinc-finger transcription factor, is required for full induction of clonal anergy in CD4+ T cells. J. Immunol. *173*, 7331–7338.

He, X.S., Rehermann, B., Lopez-Labrador, F.X., Boisvert, J., Cheung, R., Mumm, J., Wedemeyer, H., Berenguer, M., Wright, T.L., Davis, M.M., and Greenberg, H.B. (1999). Quantitative analysis of hepatitis C virus-specific CD8(+) T cells in peripheral blood and liver using peptide-MHC tetramers. Proc. Natl. Acad. Sci. USA *96*, 5692–5697.

Heissmeyer, V., Macian, F., Im, S.H., Varma, R., Feske, S., Venuprasad, K., Gu, H., Liu, Y.C., Dustin, M.L., and Rao, A. (2004). Calcineurin imposes T cell unresponsiveness through targeted proteolysis of signaling proteins. Nat. Immunol. *5*, 255–265.

Intlekofer, A.M., Takemoto, N., Wherry, E.J., Longworth, S.A., Northrup, J.T., Palanivel, V.R., Mullen, A.C., Gasink, C.R., Kaech, S.M., Miller, J.D., et al. (2005). Effector and memory CD8+ T cell fate coupled by T-bet and eomesodermin. Nat. Immunol. *6*, 1236–1244.

Joshi, N.S., Cui, W., Chandele, A., Lee, H.K., Urso, D.R., Hagman, J., Gapin, L., and Kaech, S.M. (2007). Inflammation directs a gradient of T-bet expression that specifies memory precursor and short-lived effector CD8 T cell fates. Immunity *27*, 281–295.

Kabashima, K., Saji, T., Murata, T., Nagamachi, M., Matsuoka, T., Segi, E., Tsuboi, K., Sugimoto, Y., Kobayashi, T., Miyachi, Y., et al. (2002). The prostaglandin receptor EP4 suppresses colitis, mucosal damage and CD4 cell activation in the gut. J. Clin. Invest. *109*, 883–893.

Kaech, S.M., Hemby, S., Kersh, E., and Ahmed, R. (2002). Molecular and functional profiling of memory CD8 T cell differentiation. Cell *111*, 837–851.

Kallies, A., Hawkins, E.D., Belz, G.T., Metcalf, D., Hommel, M., Corcoran, L.M., Hodgkin, P.D., and Nutt, S.L. (2006). Transcriptional repressor Blimp-1 is essential for T cell homeostasis and self-tolerance. Nat. Immunol. *7*, 466–474.

Katz, H.R., Vivier, E., Castells, M.C., McCormick, M.J., Chambers, J.M., and Austen, K.F. (1996). Mouse mast cell gp49B1 contains two immunoreceptor tyrosine-based inhibition motifs and suppresses mast cell activation when coligated with the high-affinity Fc receptor for IgE. Proc. Natl. Acad. Sci. USA *93*, 10809–10814.

Kuo, C.T., Veselits, M.L., and Leiden, J.M. (1997). LKLF: A transcriptional regulator of single-positive T cell quiescence and survival. Science *277*, 1986–1990.

Lanier, L.L. (1998). NK cell receptors. Annu. Rev. Immunol. *16*, 359–393.

Liu, N., Phillips, T., Zhang, M., Wang, Y., Opferman, J.T., Shah, R., and Ashton-Rickardt, P.G. (2004). Serine protease inhibitor 2A is a protective factor for memory T cell development. Nat. Immunol. *5*, 919–926.

Macian, F., Garcia-Cozar, F., Im, S.H., Horton, H.F., Byrne, M.C., and Rao, A. (2002). Transcriptional mechanisms underlying lymphocyte tolerance. Cell *109*, 719–731.

Maeda, M., Carpenito, C., Russell, R.C., Dasanjh, J., Veinotte, L.L., Ohta, H., Yamamura, T., Tan, R., and Takei, F. (2005). Murine CD160, Ig-like receptor on NK cells and NKT cells, recognizes classical and nonclassical MHC class I and regulates NK cell activation. J. Immunol. *175*, 4426–4432.

Martins, G.A., Cimmino, L., Shapiro-Shelef, M., Szabolcs, M., Herron, A., Magnusdottir, E., and Calame, K. (2006). Transcriptional repressor Blimp-1 regulates T cell homeostasis and function. Nat. Immunol. *7*, 457–465.

Masopust, D., Ha, S.J., Vezys, V., and Ahmed, R. (2006). Stimulation history dictates memory CD8 T cell phenotype: Implications for prime-boost vaccination. J. Immunol. *177*, 831–839.

Mueller, D.L. (2004). E3 ubiquitin ligases as T cell anergy factors. Nat. Immunol. *5*, 883–890.

Ou, R., Zhou, S., Huang, L., and Moskophidis, D. (2001). Critical role for alpha/beta and gamma interferons in persistence of lymphocytic choriomeningitis virus by clonal exhaustion of cytotoxic T cells. J. Virol. *75*, 8407–8423.

Parry, R.V., Chemnitz, J.M., Frauwirth, K.A., Lanfranco, A.R., Braunstein, I., Kobayashi, S.V., Linsley, P.S., Thompson, C.B., and Riley, J.L. (2005). CTLA-4 and PD-1 receptors inhibit T-cell activation by distinct mechanisms. Mol. Cell. Biol. *25*, 9543–9553.

Pearce, E.L., Mullen, A.C., Martins, G.A., Krawczyk, C.M., Hutchins, A.S., Zediak, V.P., Banica, M., DiCioccio, C.B., Gross, D.A., Mao, C.A., et al. (2003). Control of effector CD8+ T cell function by the transcription factor Eomesodermin. Science *302*, 1041–1043.

Petrovas, C., Casazza, J.P., Brenchley, J.M., Price, D.A., Gostick, E., Adams, W.C., Precopio, M.L., Schacker, T., Roederer, M., Douek, D.C., and Koup, R.A. (2006). PD-1 is a regulator of virus-specific CD8+ T cell survival in HIV infection. J. Exp. Med. *203*, 2281–2292.

Petrovas, C., Price, D.A., Mattapallil, J., Ambrozak, D.R., Geldmacher, C., Cecchinato, V., Vaccari, M., Tryniszewska, E., Gostick, E., Roederer, M., et al. (2007). SIV-specific CD8+T-cells express high levels of PD1 and cytokines but have impaired proliferative capacity in acute and chronic SIVmac251 infection. Blood *110*, 928–936.

Radziewicz, H., Ibegbu, C.C., Fernandez, M.L., Workowski, K.A., Obideen, K., Wehbi, M., Hanson, H.L., Steinberg, J.P., Masopust, D., Wherry, E.J., et al. (2006). Liver infiltrating lymphocytes in chronic human HCV infection display an exhausted phenotype with high PD-1 and low CD127 expression. J. Virol. *81*, 2545–2553.

Rathmell, J.C., Vander Heiden, M.G., Harris, M.H., Frauwirth, K.A., and Thompson, C.B. (2000). In the absence of extrinsic signals, nutrient utilization by lymphocytes is insufficient to maintain either cell size or viability. Mol. Cell *6*, 683–692.

Rojo, S., Burshtyn, D.N., Long, E.O., and Wagtmann, N. (1997). Type I transmembrane receptor with inhibitory function in mouse mast cells and NK cells. J. Immunol. *158*, 9–12.

Safford, M., Collins, S., Lutz, M.A., Allen, A., Huang, C.T., Kowalski, J., Blackford, A., Horton, M.R., Drake, C., Schwartz, R.H., and Powell, J.D. (2005). Egr-2 and Egr-3 are negative regulators of T cell activation. Nat. Immunol. *6*, 472–480.

Sagerstrom, C.G. (2004). PbX marks the spot. Dev. Cell *6*, 737–738.

Schwartz, R.H. (2003). T cell anergy. Annu. Rev. Immunol. *21*, 305–334.

Shin, H., Blackburn, S.D., Blattman, J.N., and Wherry, E.J. (2007). Viral antigen and extensive division maintain virus-specific CD8 T cells during chronic infection. J. Exp. Med. *204*, 941–949.

Shin, H., and Wherry, E.J. (2007). CD8 T cell dysfunction during chronic viral infection. Curr. Opin. Immunol. *19*, 408–415.

Subramanian, A., Tamayo, P., Mootha, V.K., Mukherjee, S., Ebert, B.L., Gillette, M.A., Paulovich, A., Pomeroy, S.L., Golub, T.R., Lander,

E.S., and Mesirov, J.P. (2005). Gene set enrichment analysis: A knowledge-based approach for interpreting genome-wide expression profiles. Proc. Natl. Acad. Sci. USA *102*, 15545–15550.

Surh, C.D., Boyman, O., Purton, J.F., and Sprent, J. (2006). Homeostasis of memory T cells. Immunol. Rev. *211*, 154–163.

Trautmann, L., Janbazian, L., Chomont, N., Said, E.A., Gimmig, S., Bessette, B., Boulassel, M.R., Delwart, E., Sepulveda, H., Balderas, R.S., et al. (2006). Upregulation of PD-1 expression on HIV-specific CD8+ T cells leads to reversible immune dysfunction. Nat. Med. *12*, 1198–1202.

Urbani, S., Amadei, B., Tola, D., Massari, M., Schivazappa, S., Missale, G., and Ferrari, C. (2006). PD-1 expression in acute hepatitis C virus (HCV) infection is associated with HCV-specific CD8 exhaustion. J. Virol. *80*, 11398–11403.

van Lier, R.A., ten Berge, I.J., and Gamadia, L.E. (2003). Human CD8(+) T-cell differentiation in response to viruses. Nat. Rev. Immunol. *3*, 931–939.

Velu, V., Kannanganat, S., Ibegbu, C., Chennareddi, L., Villinger, F., Freeman, G.J., Ahmed, R., and Amara, R.R. (2007). Elevated expression levels of inhibitory receptor programmed death 1 on simian immunodeficiency virus-specific CD8 T cells during chronic infection but not after vaccination. J. Virol. *81*, 5819–5828.

Voehringer, D., Blaser, C., Brawand, P., Raulet, D.H., Hanke, T., and Pircher, H. (2001). Viral infections induce abundant numbers of senescent CD8 T cells. J. Immunol. *167*, 4838–4843.

Watanabe, N., Gavrieli, M., Sedy, J.R., Yang, J., Fallarino, F., Loftin, S.K., Hurchla, M.A., Zimmerman, N., Sim, J., Zang, X., et al. (2003). BTLA is a lymphocyte inhibitory receptor with similarities to CTLA-4 and PD-1. Nat. Immunol. *4*, 670–679.

Wherry, E.J., and Ahmed, R. (2004). Memory CD8 T-cell differentiation during viral infection. J. Virol. *78*, 5535–5545.

Wherry, E.J., Barber, D.L., Kaech, S.M., Blattman, J.N., and Ahmed, R. (2004). Antigen-independent memory CD8 T cells do not develop during chronic viral infection. Proc. Natl. Acad. Sci. USA *101*, 16004–16009.

Wherry, E.J., Blattman, J.N., and Ahmed, R. (2005). Low CD8 T-cell proliferative potential and high viral load limit the effectiveness of therapeutic vaccination. J. Virol. *79*, 8960–8968.

Wherry, E.J., Blattman, J.N., Murali-Krishna, K., van der Most, R., and Ahmed, R. (2003). Viral persistence alters CD8 T-cell immunodominance and tissue distribution and results in distinct stages of functional impairment. J. Virol. *77*, 4911–4927.

Workman, C.J., Dugger, K.J., and Vignali, D.A. (2002). Cutting edge: Molecular analysis of the negative regulatory function of lymphocyte activation gene-3. J. Immunol. *169*, 5392–5395.

Zajac, A.J., Blattman, J.N., Murali-Krishna, K., Sourdive, D.J., Suresh, M., Altman, J.D., and Ahmed, R. (1998). Viral immune evasion due to persistence of activated T cells without effector function. J. Exp. Med. *188*, 2205–2213.

Zhang, J.Y., Zhang, Z., Wang, X., Fu, J.L., Yao, J., Jiao, Y., Chen, L., Zhang, H., Wei, J., Jin, L., et al. (2007). PD-1 upregulation is correlated with HIV-specific memory CD8+ T-cell exhaustion in typical progressors, but not in long-term non-progressors. Blood *109*, 4671–4678.

Accession Numbers

The gene-expression data described in this paper have been deposited in the NCBI's Gene Expression Omnibus and are accessible through GEO accession numbers GSM235537-GSM235551.